PHYSICAL REVIEW B VOLUME 53, NUMBER 7 15 FEBRUARY 1996-I

Exchange-correlation energy of a quasi-two-dimensional electron gas: A Hartree self-consistent approach

M. Combescot, O. Betbeder-Matibet, and C. Benoit a la Guillaume
Groupe de Physique des Solides, Université Denis Diderot and Université Pierre et Marie Curie, CNRS URA 17, Tour 23,
2 place Jussieu, 75251 Paris Cedex 05, France

(Received 14 July 1995)

We present an approach to the exchange-correlation energy of an electron gas confined in a finite-width quantum well, which avoids the local-density approximation. We focus on densities large enough to have electrons in more than one subband. This imposes a self-consistent treatment of the Hartree interaction (i.e., $q=0$ excitation processes) while the $q\neq 0$ interaction can be treated perturbatively. By writing the Hamiltonian in terms of appropriate Hartree self-consistent creation operators, we can cancel most but not all $q=0$ Coulomb contributions; a few mixed $(q=0,q\neq 0)$ terms do remain in the correlation energy. A numerical calculation of the exchange energy shows that the effect of the Hartree processes turns out to stay rather small in the whole two-subband filling domain.

In recent publications,[1,2] we have studied the Hartree, exchange, and correlation energies of a quasi-two-dimensional electron gas localized in a quantum well. We have shown that for a well width smaller than the Bohr radius and electrons in the lowest subband only, it is unnecessary to calculate the Hartree energy in a self-consistent way, its perturbative expansion with one or possibly two terms already providing a very accurate result.[1] Within this simplification it is possible to avoid the local density approximation[3–6] for the exchange-correlation energy and to treat this contribution as well as the Hartree part through a perturbative treatment of the Coulomb interaction, similar to the one used for three-dimensional (3D) and exact 2D electron gases. This approach allows an easy derivation of the well width dependence of all terms.[2]

In the present work, we turn to situations, such as electrons in more than one subband, for which the Hartree energy has to be calculated in a self-consistent way. We again avoid the usual treatment of exchange and correlation effects through the local density approximation, and concentrate on cases for which the well width and electron density are both large enough to impose a self-consistent treatment of all Hartree processes, while the exchange and correlation processes can still be treated perturbatively.[7–9]

It is important to stress that a many-subband filling gives rise to an additional complexity since the fillings[10] depend on the Coulomb interaction: Indeed, the Hartree processes modify the subband bottom energies and thus the number of electrons in each subband at equilibrium. These fillings enter the Hartree energy as well as the exchange-correlation contributions, and thus modify their values accordingly.

In view of all these complexities, we found it interesting and useful to first derive the Hartree energy from two different approaches.

(i) In the first approach, we start as in Ref. 1: We write the Hamiltonian in terms of creation operators $a^\dagger_{n\mathbf{k}}$ for *free* electrons in the well. The part of the Coulomb interaction with zero momentum transfers (called Hartree processes) is expanded perturbatively and summed up to all orders. This infinite summation yields the Hartree energy. It can be performed using standard technics for many-body problems.[11] We however show that for electrons in more than one subband, this summation cannot be done with $T=0$ Green's functions but imposes the finite T formalism.

(ii) In the second approach, we start completely differently. We introduce a so-called Hartree basis composed of the eigenstates of a Poisson-Schrödinger Hamiltonian. We use this basis to define new creation operators $A^\dagger_{n\mathbf{k}}$ and we write the total Hamiltonian in terms of these operators. We then split this total Hamiltonian into a one-body diagonal part and a two-body part composed of new zero momentum $(q=0)$ and nonzero momentum $(q\neq 0)$ excitation processes. We show that for the equilibrium fillings of the Hartree problem, the contributions of these new $(q=0)$ processes to the Hartree energy cancel so that the exact Hartree energy is simply given by the one-body diagonal part of the Hamiltonian.

This second approach turns out to be quite appropriate to derive the exchange-correlation energy in an easy way. With the Hamiltonian now written in terms of $A^\dagger_{n\mathbf{k}}$ Hartree operators, we find that most of the usual mixed $(q=0,q\neq 0)$ terms cancel, so that the Coulomb expansion of the energy is greatly simplified when compared to the standard approach in terms of $a^\dagger_{n\mathbf{k}}$ free-electron operators. In particular, all the mixed $(q=0,q\neq 0)$ processes of the exchange energy give zero, while the first correlation term [i.e., the term quadratic in $(q\neq 0)$ processes] contains one mixed Hartree-correlation contribution only.

The paper is organized as follows.

In Sec. I, we recall the formalism of Refs. 1 and 2, and give the range of parameters for which a self-consistent treatment of the Hartree energy is necessary while the exchange-correlation energy can be calculated perturbatively. We then derive the Hartree energy from the first approach described above, using free-electron operators.

In Sec. II, we rewrite the total Hamiltonian in terms of Hartree creation operators defined on a Hartree basis and we show how we can recover the Hartree energy obtained in Sec. I.

0163-1829/96/53(7)/3861(18)/$06.00

In Sec. III, we use the expression of the finite momentum transfer Coulomb interaction obtained in Sec. II, to derive the exchange energy, the mixed Hartree-exchange energy, the second-order correlation energy, and the mixed Hartree–second-order correlation energy.

In Sec. IV, we have gathered all numerical results. The self-consistent treatment of the Hartree processes implies the resolution of a Poisson-Schrödinger equation which cannot be solved but numerically. Moreover, the solutions of this equation depend on the ion distribution in a nontrivial way. In order to illustrate the Hartree self-consistent approach exposed in Secs. II and III, we have chosen a configuration with ions on both sides of the electron layer and we have considered two different well widths. In the first part, we give the subband fillings, energies, and wave functions, taking into account Hartree processes only. We then calculate the Hartree energy and exchange energy as functions of the electron density and we discuss the effect of the well width on these quantities. We also give the electron-hole chemical potential of a doped quantum well as induced by this Hartree self-consistent approach.

I. HARTREE ENERGY WITHIN THE FREE-ELECTRON BASIS

A. Hamiltonians

The one-particle Hamiltonian for free electrons in a quantum well of surface S and width a reads

$$h=h_{xy}+h_z=\frac{p_x^2+p_y^2}{2m}+\left[\frac{p_z^2}{2m}+u(z)\right], \tag{1.1}$$

where $u(z)$ is the well potential. Let $|\mathbf{k}\rangle$ be the h_{xy} eigenstates of energy ε_k,[12]

$$h_{xy}|\mathbf{k}\rangle=\varepsilon_k|\mathbf{k}\rangle, \quad \varepsilon_k=\frac{k^2}{2m},$$

$$\langle\rho|\mathbf{k}\rangle=e^{i\mathbf{k}\cdot\boldsymbol{\rho}}/\sqrt{S}, \quad \rho=(x,y), \tag{1.2}$$

and $|\varphi_n\rangle$ the h_z eigenstate of energy ε_n,

$$h_z|\varphi_n\rangle=\varepsilon_n|\varphi_n\rangle. \tag{1.3}$$

For infinite well barriers at $z=0$ and $z=a$, we have

$$\langle z|\varphi_n\rangle=\varphi_n(z)=(2/a)^{1/2}\sin(n\pi z/a),$$

$$\varepsilon_n=\frac{\pi^2n^2}{2ma^2}. \tag{1.4}$$

The $|\varphi_{n\mathbf{k}}\rangle$ eigenstates of h are given by

$$|\varphi_{n\mathbf{k}}\rangle=|\varphi_n\rangle\otimes|\mathbf{k}\rangle,$$

$$h|\varphi_{n\mathbf{k}}\rangle=(\varepsilon_n+\varepsilon_k)|\varphi_{n\mathbf{k}}\rangle. \tag{1.5}$$

Using these $|\varphi_{n\mathbf{k}}\rangle$ states as a basis for second quantization, and calling $a_{n\mathbf{k}\sigma}^\dagger$ the corresponding creation operators (σ being the spin index), the free electron part of the N electron Hamiltonian appears in a diagonal form and reads

$$\mathscr{H}_0=\sum_{n\mathbf{k}\sigma}(\varepsilon_n+\varepsilon_k)a_{n\mathbf{k}\sigma}^\dagger a_{n\mathbf{k}\sigma}. \tag{1.6}$$

We now consider the *total* Coulomb interaction[12] between N electrons at $\mathbf{r}_n$ $(n=1,N)$ and N ions assumed to be delocalized in a quasi-2D jellium with density $n_i(\mathbf{r})=\rho_i(z)N/S$,

$$\mathscr{V}_{\text{coul}}=\frac{1}{2}\sum_{n\neq n'}\frac{e^2}{|\mathbf{r}_n-\mathbf{r}_{n'}|}+\frac{1}{2}\int\int d^3r\,d^3r'\,\frac{e^2}{|\mathbf{r}-\mathbf{r}'|}n_i(\mathbf{r})n_i(\mathbf{r}')$$
$$-\sum_n\int d^3r\frac{e^2}{|\mathbf{r}-\mathbf{r}_n|}n_i(\mathbf{r}). \tag{1.7}$$

When written in second quantization with the $|\varphi_{n\mathbf{k}}\rangle$ basis, this Hamiltonian can be split into two parts,

$$\mathscr{V}_{\text{coul}}=\mathscr{V}^{(q=0)}+\mathscr{V}^{(q\neq0)}. \tag{1.8}$$

The zero momentum transfer part reads[1]

$$\mathscr{V}^{(q=0)}=\frac{1}{2}\frac{2\pi e^2}{Sa^{-1}}\sum_{\substack{n_1n_1'\\n_2n_2'}}\sum_{\substack{\mathbf{k}_1\sigma_1\\\mathbf{k}_2\sigma_2}}w_{n_1n_1';n_2n_2'}a_{n_1\mathbf{k}_1\sigma_1}^\dagger a_{n_2\mathbf{k}_2\sigma_2}^\dagger$$
$$\times a_{n_2'\mathbf{k}_2\sigma_2}a_{n_1'\mathbf{k}_1\sigma_1}, \tag{1.9}$$

$$w_{n_1n_1';n_2n_2'}=-\int\int dz_1dz_2\frac{|z_1-z_2|}{a}$$
$$\times[\varphi_{n_1}^*(z_1)\varphi_{n_1'}(z_1)-\rho_i(z_1)\delta_{n_1n_1'}]$$
$$\times[\varphi_{n_2}^*(z_2)\varphi_{n_2'}(z_2)-\rho_i(z_2)\delta_{n_2n_2'}], \tag{1.10}$$

while the finite momentum transfer part reads[2]

$$\mathscr{V}^{(q\neq0)}=\frac{1}{2}\sum_{\mathbf{q}\neq0}\frac{2\pi e^2}{Sq}\sum_{\substack{n_1n_1'\\n_2n_2'}}\sum_{\substack{\mathbf{k}_1\sigma_1\\\mathbf{k}_2\sigma_2}}v_{n_1n_1';n_2n_2'}(q)$$
$$\times a_{n_1\mathbf{k}_1+\mathbf{q}\sigma_1}^\dagger a_{n_2\mathbf{k}_2-\mathbf{q}\sigma_2}^\dagger a_{n_2'\mathbf{k}_2\sigma_2}a_{n_1'\mathbf{k}_1\sigma_1}, \tag{1.11}$$

$$v_{n_1n_1';n_2n_2'}(q)=\int\int dz_1dz_2e^{-q|z_1-z_2|}\varphi_{n_1}^*(z_1)\varphi_{n_1'}(z_1)$$
$$\times\varphi_{n_2}^*(z_2)\varphi_{n_2'}(z_2). \tag{1.12}$$

B. Range of parameters implying a self-consistent treatment of the Hartree terms

The properties of a quasi-2D electron gas confined in a quantum well depend on the well width a, the ion configuration $\rho_i(z)$, and the 2D electron density

$$n_s=\frac{N}{S}=\frac{K^2}{2\pi}. \tag{1.13}$$

From n_s, we can construct the usual dimensionless parameter r_s, which reads

$$n_s\pi r_s^2a_0^2=1\Rightarrow r_s=\sqrt{2}/Ka_0, \tag{1.14}$$

where $a_0 = 1/me^2$ is the Bohr radius.[12] By similarity with the 3D case, a perturbative expansion of the Coulomb energy in $\mathcal{V}^{(q\neq 0)}$ is valid for dense systems only, i.e., for $r_s < 1$.

With respect to the $\mathcal{V}^{(q=0)}$ expansion of the Hartree energy, we have shown[1] that it is controlled by a dimensionless parameter λ_H, which is proportional to e^2 and n_s, and is explicitly given by[13]

$$\lambda_H = \frac{K^2 a^3}{\pi^4 a_0} = \frac{2}{\pi^4}\left(\frac{a}{a_0}\right)^3 \frac{1}{r_s^2}. \qquad (1.15)$$

A perturbative expansion of the Hartree energy is thus valid for

$$\lambda_H < 1 \Rightarrow \frac{a}{a_0} < \left(\frac{\pi^4}{2} r_s^2\right)^{1/3}. \qquad (1.16)$$

Let us now consider the subband filling in the absence of Coulomb interaction: The electrons occupy *one* subband only if

$$\varepsilon_1 + \varepsilon_K < \varepsilon_2 \Rightarrow \frac{a}{a_0} < \sqrt{\tfrac{3}{2}}\,\pi r_s. \qquad (1.17)$$

They occupy *two* subbands, with N_1^0 (N_2^0) electrons in the $n=1$ ($n=2$) subband, if

$$N_1^0 = S(K_1^0)^2/2\pi, \quad N_2^0 = S(K_2^0)^2/2\pi = N - N_1^0,$$

$$\varepsilon_1 + \varepsilon_{K_1^0} = \varepsilon_2 + \varepsilon_{K_2^0}. \qquad (1.18)$$

This implies

$$\varepsilon_2 - \varepsilon_1 < \varepsilon_K < 2\varepsilon_3 - \varepsilon_1 - \varepsilon_2 \Rightarrow \sqrt{\tfrac{3}{2}}\,\pi r_s < \frac{a}{a_0} < \sqrt{\tfrac{13}{2}}\,\pi r_s. \qquad (1.19)$$

In the same way, we find that the electrons occupy *three* subbands if

$$\sqrt{\tfrac{13}{2}}\,\pi r_s < \frac{a}{a_0} < \sqrt{17}\,\pi r_s \qquad (1.20)$$

and so on.

The ranges of parameters a/a_0 versus r_s corresponding to one-, two-, and three-subband fillings, are shown in Fig. 1. In this figure we have also shown the $\lambda_H = 1$ curve. If we restrict ourselves to the $r_s < 1$ domain, in order to allow a reliable calculation of the exchange-correlation energy, we see that most of the one-subband domain and a small part of the two-subband domains lie below the $\lambda_H = 1$ curve while all other filling situations correspond to $\lambda_H > 1$.

In our preceding works, we have considered electrons in the lowest subband only, for which we essentially have $\lambda_H < 1$ if $r_s < 1$: a perturbative expansion of the Coulomb energy in $\mathcal{V}^{(q\neq 0)}$ *and* $\mathcal{V}^{(q=0)}$ is thus expected to be valid in this case. Indeed, we have checked that the perturbative expansion of the Hartree energy, with only one or possibly two terms, gives a result very close to its exact value obtained by solving self-consistently the usual Poisson-Schrödinger equation.

In this paper we wish to turn to a more difficult problem: Our goal is to calculate the exchange-correlation energy in a 3D-like way, i.e., as an expansion in $\mathcal{V}^{(q\neq 0)}$, whereas performing a summation of all the $q=0$ processes. As shown in Fig. 1, this is necessary when electrons fill more than one subband, since in this case $\lambda_H > 1$ for $r_s < 1$. For simplicity we will concentrate here on situations where electrons occupy the two lowest subbands only (the extension to electrons filling more than two subbands being formally straightforward). For a well width $a = 3a_0$, the two-subband filling corresponds to $0.37 < r_s < 0.78$ and $0.91 < \lambda_H < 3.95$.

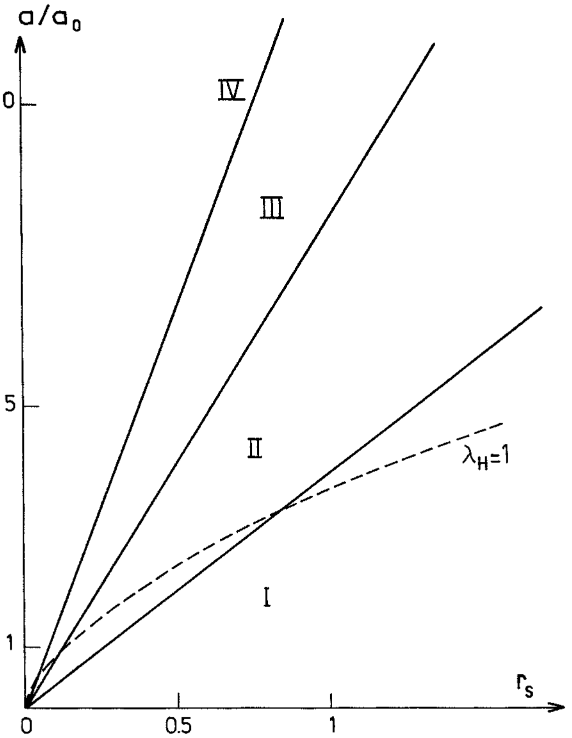

FIG. 1. a/a_0 versus r_s domains for which electrons fill one (I), two (II), three (III), etc. subbands. The dashed curve corresponds to $\lambda_H = 1$.

C. Calculation of the Hartree energy by summing all $q=0$ processes

The Hartree energy is the ground-state energy of $\mathcal{H}_H$, defined as

$$\mathcal{H}_H = \mathcal{H}_0 + \mathcal{V}^{(q=0)}. \qquad (1.21)$$

The perturbative expansion of this energy corresponds to all possible diagrams with $q=0$ transfers only. These are shown in Fig. 2(a), up to third order in $\mathcal{V}^{(q=0)}$. The first two terms have been explicitly calculated in Ref. 1.

1. Method

If we want to sum up all these terms, the Green's function approach seems a well adapted procedure. However, in the case of electrons in more than one subband, the $T=0$ Green's functions cannot be used for the following reason: it is stated at a very early stage of the theory, that the $T=0$ Green's function formalism applies to problems in which the perturbed ground state derives from the unperturbed one. This is not the case if electrons are in two subbands. Indeed

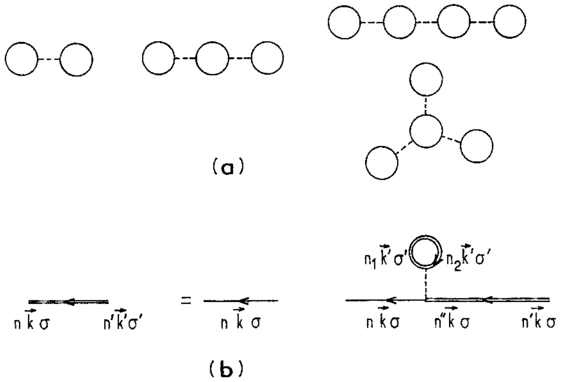

FIG. 2. (a) Hartree energy diagrams up to second order in $\mathscr{V}^{(q=0)}$ interaction (dashed line). (b) Electron propagator renormalized by the Hartree interaction.

the subband filling in the absence of Coulomb interaction corresponds to N_1^0 and N_2^0 given by Eq. (1.18). In the presence of $\mathscr{V}^{(q=0)}$, we expect the subband bottom energies to be modified from $\varepsilon_1,\varepsilon_2$ to E_1,E_2, so that the equilibrium fillings N_1,N_2 should now verify

$$N_1=SK_1^2/2\pi, \quad N_2=SK_2^2/2\pi=N-N_1,$$

$$E_1+\varepsilon_{K_1}=E_2+\varepsilon_{K_2}. \tag{1.22}$$

The $T=0$ formalism would in fact give the properties of a perturbed state with N_1^0 and N_2^0 electrons in the two lowest subbands and not those of the true Hartree ground state.

If we use instead finite-T Green's functions,[11] and let T go to zero at the end, we must clearly generate the correct "perturbed" ground state. The bare propagator then reads[11]

$$g_n(k,\omega_\nu)=\frac{1}{i\omega_\nu+\mu-\varepsilon_k-\varepsilon_n} \tag{1.23}$$

with $\omega_\nu=(2\nu+1)\pi T$, v being an integer. The $\mathscr{V}^{(q=0)}$ interaction renormalizes this bare propagator. Using the standard $T\neq 0$ Green's function procedure we find that the renormalized propagator verifies the following Dyson equation [see Fig. 2(b)]:

$$\mathscr{G}_{nn'}(k,\omega_\nu)=g_n(k,\omega_\nu)\delta_{nn'}$$
$$+g_n(k,\omega_\nu)\sum_{n''}\sigma_{nn''}\mathscr{G}_{n''n'}(k,\omega_\nu), \tag{1.24}$$

where the self-energy $\sigma_{nn'}$ induced by the Hartree potential is independent of k and ω_ν. It is precisely given by

$$\sigma_{nn'}=\frac{2\pi e^2}{Sa^{-1}}\sum_{n_1n_2} w_{nn';n_1n_2}\mathscr{N}_{n_2n_1}, \tag{1.25}$$

$$\mathscr{N}_{n_2n_1}=\lim_{\tau\to 0^+} T\sum_{\nu\mathbf{k}\sigma} e^{i\omega_\nu\tau}\mathscr{G}_{n_2n_1}(k,\omega_\nu). \tag{1.26}$$

At fixed temperature T and chemical potential μ, the average energy $\bar{\mathscr{E}}_H(\mu,T)$, electron number $\bar{N}(\mu,T)$, and electron density $\bar{n}(z,\mu,T)$ can be expressed in terms of the renormalized Green's functions:[11]

$$\bar{\mathscr{E}}_H(\mu,T)=\frac{1}{2}\lim_{\tau\to 0^+} T\sum_{\nu n\mathbf{k}\sigma} e^{i\omega_\nu\tau}$$
$$\times(i\omega_\nu+\mu+\varepsilon_k+\varepsilon_n)\mathscr{G}_{nn}(k,\omega_\nu), \tag{1.27}$$

$$\bar{N}(\mu,T)=\sum_n \mathscr{N}_{nn} \tag{1.28}$$

$$\bar{n}(z,\mu,T)=\lim_{\tau\to 0^+} T\sum_{\nu nn'} e^{i\omega_\nu\tau}\varphi_n(z)\varphi_{n'}^*(z)\mathscr{G}_{nn'}(k,\omega_\nu). \tag{1.29}$$

Equation (1.28) will allow to determine μ as a function of N and T by setting as usual

$$\bar{N}(\mu,T)=N. \tag{1.30}$$

2. Resolution of the Dyson equation

We now turn to the resolution of Eq. (1.24). We first note that the bare Green's function given by Eq. (1.23) can be related to the following operator g:

$$g=\frac{1}{i\omega_\nu+\mu-\varepsilon_k-h_z}, \tag{1.31}$$

where h_z is the Hamiltonian defined in Eq. (1.1). From (1.3) and (1.23) we obviously get

$$\langle\varphi_n|g|\varphi_{n'}\rangle=g_n(k,\omega_\nu)\delta_{nn'}. \tag{1.32}$$

Let us introduce in the same way the operators G and σ_z defined by

$$\langle\varphi_n|G|\varphi_{n'}\rangle=\mathscr{G}_{nn'}(k,\omega_\nu), \tag{1.33}$$

$$\langle\varphi_n|\sigma_z|\varphi_{n'}\rangle=\sigma_{nn'}. \tag{1.34}$$

Equation (1.24) then simply reads

$$G=g+g\sigma_z G. \tag{1.35}$$

Inserting Eq. (1.31) into Eq. (1.35), we get

$$G^{-1}=g^{-1}-\sigma_z=(i\omega_\nu+\mu-\varepsilon_k-H_z), \tag{1.36}$$

where H_z, defined by

$$H_z=h_z+\sigma_z, \tag{1.37}$$

can be seen as a z Hamiltonian in the presence of Hartree interaction. The operator G is thus formally similar to g and reads

$$G=\frac{1}{i\omega_\nu+\mu-\varepsilon_k-H_z}. \tag{1.38}$$

Let $|\phi_n\rangle$ be the eigenstates of H_z,

$$H_z|\phi_n\rangle=E_n|\phi_n\rangle. \tag{1.39}$$

The $|\phi_n\rangle$ form an orthonormal basis since H_z, like h_z, are Hermitian. In this $|\phi_n\rangle$ basis, the operator G is diagonal and its matrix elements simply read

$$\langle \phi_n|G|\phi_{n'}\rangle=\frac{\delta_{nn'}}{i\omega_\nu+\mu-\varepsilon_k-E_n}=G_n(k,\omega_\nu)\,\delta_{nn'}. \tag{1.40}$$

From them, we easily deduce the G matrix elements in the $|\varphi_n\rangle$ basis,

$$\mathscr{G}_{nn'}(k,\omega_\nu)=\sum_{n''}\langle\varphi_n|\phi_{n''}\rangle\langle\phi_{n''}|\varphi_{n'}\rangle G_{n''}(k,\omega_\nu). \tag{1.41}$$

3. Link with the Poisson-Schrödinger equation

Before going further, let us study this $|\phi_n\rangle$ basis. We expect it to be related to the eigenstates of the Poisson-Schrödinger equation appearing in the standard derivation of the Hartree energy.

From the definitions of $\sigma_{nn'}$ [Eq. (1.25)] and $\bar{n}(z,\mu,T)$ [Eq. (1.29)], we can show (see Appendix A) that σ_z is given by

$$\sigma_z=V_z-\int dz V_z\rho_i(z), \tag{1.42}$$

where V_z is the electrostatic energy of an electron in the presence of a charge distribution $en_s[\rho_i(z)-\rho_e(z)]$

$$V_z=-2\pi e^2 n_s\int dz'|z-z'|[\rho_e(z')-\rho_i(z')] \tag{1.43}$$

provided that $\rho_e(z)$ is defined as

$$\rho_e(z)=\frac{1}{N}\bar{n}(z,\mu,T)=\sum_n \frac{N_n}{N}|\phi_n(z)|^2, \tag{1.44}$$

where the N_n are given in terms of the G_n by

$$N_n=\lim_{\tau\to 0^+} T\sum_{\nu\mathbf{k}\sigma} e^{i\omega_\nu\tau}G_n(k,\omega_\nu). \tag{1.45}$$

We see, from Eq. (1.42), that σ_z and V_z differ by a constant independent of z.

Using Eqs. (1.37), (1.39), and (1.42), we deduce that the $|\phi_n\rangle$ also verify

$$\hat{H}_z|\phi_n\rangle=\hat{E}_n|\phi_n\rangle,$$

$$\hat{H}_z=h_z+V_z, \tag{1.46}$$

where the new eigenvalues $\hat{E}_n$ differ from E_n by a constant term, independent of n,

$$\hat{E}_n=E_n+\int dz\ V_z\rho_i(z). \tag{1.47}$$

Equation (1.46) is nothing but the usual Poisson-Schrödinger equation of the Hartree problem.

In order to make the complete identification with the Poisson-Schrödinger approach, we must relate the N_n appearing in $\rho_e(z)$ and defined by Eq. (1.45) to the number of electrons in the renormalized subbands. Let us recall that, up to now, these N_n depend on μ and T. Inserting Eq. (1.40) into Eq. (1.45) and using the relation[11]

$$\lim_{T\to 0}\ \lim_{\tau\to 0^+} T\sum_\nu \frac{e^{i\omega_\nu\tau}}{i\omega_\nu+x}=\lim_{T\to 0}\frac{1}{1+e^{-x/T}}=\theta(x), \tag{1.48}$$

where $\theta(x)$ is the Heaviside function, we find

$$N_n(\mu,T=0)=\sum_{\mathbf{k}\sigma}\theta(\mu-\varepsilon_k-E_n), \tag{1.49}$$

so that, in the $T=0$ limit, N_n is indeed the number of electrons in the renormalized n subband with energies $(E_n+\varepsilon_k)$, up to a chemical potential μ.

In order to determine this chemical potential for a given N in the $T=0$ limit, we use Eq. (1.30). Since the trace of a matrix does not depend on the basis, Eq. (1.28) also reads

$$\bar{N}(\mu,T)=\sum_n N_n(\mu,T) \tag{1.50}$$

so that $\mu(N,T=0)$ is such that

$$N=\sum_{n\mathbf{k}\sigma}\theta(\mu(N,0)-\varepsilon_k-E_n). \tag{1.51}$$

In the case of a two-subband filling, we can verify, using Eqs. (1.49) and (1.51) that N_1 and N_2 are indeed given by Eq. (1.22). From Eq. (1.51) we also deduce the condition for a two- (renormalized) subband occupation which now reads

$$E_2-E_1<\varepsilon_K<2E_3-E_1-E_2. \tag{1.52}$$

It is somewhat different from Eq. (1.19) due to the introduction of renormalized subband energies E_n instead of ε_n.

We can note that the condition for equilibrium filling [Eq. (1.22)], as well as the condition for two-subband occupation [Eq. (1.52)] could as well be written with the E_n replaced by the Poisson-Schrödinger eigenvalues $\hat{E}_n$, since these quantities differ by a constant independent of n. We must however stress that, due to Eq. (1.51), it is E_n and not $\hat{E}_n$ which is the energy directly related to the chemical potential μ, this μ being the energy necessary to add one electron and one ion to the N electron-ion system.

Equation (1.46) is a self-consistent equation for the ϕ_n, since V_z depends on the $\phi_n(z)$ and on the E_n through the N_n, so that its solution can only be obtained numerically. The corresponding results will be given in Sec. IV.

4. Hartree energy

Let us end this section by calculating the average energy in the $T=0$ limit. From Eqs. (1.27), (1.40), and (1.41), we get

$$\bar{\mathscr{E}}_H(\mu,T)=\lim_{\tau\to 0^+} T\sum_\nu e^{i\omega_\nu\tau}\sum_{n\mathbf{k}\sigma}\frac{1}{2}\times\left[\frac{\langle\phi_n|2\varepsilon_k+h_z+H_z|\phi_n\rangle}{i\omega_\nu+\mu-\varepsilon_k-E_n}+1\right]. \tag{1.53}$$

Using Eq. (1.48) and the following relation:[11]

$$\lim_{\tau\to 0^+}\sum_\nu e^{i\omega_\nu\tau}=0, \tag{1.54}$$

we find

$$\bar{\mathcal{E}}_H(\mu,0)=\sum_{n\mathbf{k}\sigma}\langle\phi_n|\varepsilon_k+H_z-\tfrac{1}{2}\sigma_z|\phi_n\rangle\theta(\mu-\varepsilon_k-E_n). \tag{1.55}$$

With Eqs. (1.39), (1.42), and (1.49) we can rewrite this energy in terms of E_n, N_n, and $\phi_n(z)$ as

$$\mathcal{E}_H=\frac{\pi}{2mS}\sum_n N_n^2+\sum_n N_nE_n+NE, \tag{1.56}$$

$$E=\pi e^2 n_s\int\int dz\;dz'|z-z'|[\rho_e(z)-\rho_i(z)]\times[\rho_e(z')-\rho_i(z')]. \tag{1.57}$$

The first term of Eq. (1.56) is the kinetic energy of the electrons since $N_n=SK_n^2/2\pi$. The second term is the localization energy in the presence of the Hartree interaction, while the third term takes into account the double counting of the Coulomb interaction between the average charge densities included in E_n.

If we rewrite this Hartree energy in terms of the Poisson-Schrödinger eigenvalues $\hat{E}_n$, we find as in Ref. 1:

$$\mathcal{E}_H=\frac{\pi}{2mS}\sum_n N_n^2+\sum_n N_n\hat{E}_n+N\hat{E}, \tag{1.58}$$

$$\hat{E}=\pi e^2 n_s\int\int dz\;dz'|z-z'|[\rho_e(z)\rho_e(z')-\rho_i(z)\rho_i(z')]. \tag{1.59}$$

II. HARTREE ENERGY USING HARTREE CREATION OPERATORS

A. Hartree creation operators

We may hope to avoid the summation of all $\mathcal{V}^{(q=0)}$ terms by using for second quantization an appropriate basis in which the Hartree processes are somewhat included. It can thus appear as natural to introduce a set of orthonormal one-particle states

$$|\phi_{n\mathbf{k}}\rangle=|\phi_n\rangle\otimes|\mathbf{k}\rangle, \tag{2.1}$$

in which $|\mathbf{k}\rangle$ is still an h_{xy} eigenstate of energy ε_k while the $|\phi_n\rangle$ are the eigenstates of a Poisson-Schrödinger Hamiltonian,

$$\hat{H}_z=h_z+V_z, \tag{2.2}$$

$$\hat{H}_z|\phi_n\rangle=\hat{E}_n|\phi_n\rangle, \tag{2.3}$$

h_z being given by Eq. (1.1) and V_z by Eq. (1.43). V_z depends on an electronic density $\rho_e(z)$. We choose it to be the electronic density of N electrons in $|\phi_{n\mathbf{k}}\rangle$ states, with $\mathcal{N}_n$ electrons in the n subband: More precisely, we choose

$$N\rho_e(z)=\sum_n\mathcal{N}_n|\phi_n(z)|^2 \tag{2.4}$$

with $\phi_n(z)=\langle z|\phi_n\rangle$, and

$$\sum_n\mathcal{N}_n=N. \tag{2.5}$$

At this stage, the $\mathcal{N}_n$ are just parameters, without any other constraint than Eq. (2.5). Their appropriate values will be determined later. The $|\phi_n\rangle$ depend, of course, on these $\mathcal{N}_n$.

We introduce a set of creation operators $A^\dagger_{n\mathbf{k}\sigma}$ associated to the $|\phi_{n\mathbf{k}}\rangle$ states, and we rewrite the total Hamiltonian $\mathcal{H}$ in terms of these $A^\dagger_{n\mathbf{k}\sigma}$. Using the standard second-quantization procedure, we now have

$$\mathcal{H}_0=\sum_{nn'}\sum_{\mathbf{k}\sigma}(\varepsilon_k\delta_{nn'}+\mathcal{E}_{nn'})A^\dagger_{n\mathbf{k}\sigma}A_{n'\mathbf{k}\sigma}, \tag{2.6}$$

$$\mathcal{E}_{nn'}=\int dz\;\phi_n^*(z)h_z\phi_{n'}(z) \tag{2.7}$$

so that $\mathcal{H}_0$ is still diagonal in $\mathbf{k}$ but no more in n.

Turning to the Coulomb potential, we can split it, as in Sec. I, into $q=0$ and $q\neq 0$ interactions, which formally read as Eqs. (1.9) and (1.11) with $a^\dagger$ replaced by $A^\dagger$, w by W, and v by V. Namely, we have

$$\mathcal{V}^{(q=0)}=\frac{1}{2}\frac{2\pi e^2}{Sa^{-1}}\sum_{\substack{n_1n_1'\\ n_2n_2'}}\sum_{\substack{\mathbf{k}_1\sigma_1\\ \mathbf{k}_2\sigma_2}}W_{n_1n_1';n_2n_2'}A^\dagger_{n_1\mathbf{k}_1\sigma_1}A^\dagger_{n_2\mathbf{k}_2\sigma_2}\times A_{n_2'\mathbf{k}_2\sigma_2}A_{n_1'\mathbf{k}_1\sigma_1}, \tag{2.8}$$

where W is formally identical to w [Eq. (1.10)] with $\varphi_n(z)$ replaced by $\phi_n(z)$, and similarly[14] for $\mathcal{V}^{(q\neq 0)}$ and $V_{n_1n_1';n_2n_2'}(q)$.

We now perform a set of algebraic manipulations, the purpose of which is to rewrite the Hartree Hamiltonian $\mathcal{H}_H$ [Eq. (1.21)] as

$$\mathcal{H}_H=\tilde{\mathcal{H}}_0+\tilde{\mathcal{V}}^{(q=0)}, \tag{2.9}$$

where $\tilde{\mathcal{H}}_0$ is a one-body *diagonal* Hamiltonian,

$$\tilde{\mathcal{H}}_0=\sum_{n\mathbf{k}\sigma}(\varepsilon_k+\tilde{E}_n)A^\dagger_{n\mathbf{k}\sigma}A_{n\mathbf{k}\sigma}, \tag{2.10}$$

and $\tilde{\mathcal{V}}^{(q=0)}$ a two-body interaction,

$$\tilde{\mathcal{V}}^{(q=0)}=\frac{1}{2}\frac{2\pi e^2}{Sa^{-1}}\sum_{\substack{n_1n_1'\\ n_2n_2'}}\sum_{\substack{\mathbf{k}_1\sigma_1\\ \mathbf{k}_2\sigma_2}}\tilde{W}_{n_1n_1';n_2n_2'}A^\dagger_{n_1\mathbf{k}_1\sigma_1}A^\dagger_{n_2\mathbf{k}_2\sigma_2}\times A_{n_2'\mathbf{k}_2\sigma_2}A_{n_1'\mathbf{k}_1\sigma_1}, \tag{2.11}$$

the coefficients of which verify the ''magic'' relation

$$\sum_p\mathcal{N}_p\tilde{W}_{pp;nn'}=0\quad\forall n,n'. \tag{2.12}$$

We will see later that this relation between the $\tilde{W}$ is indeed quite useful since it induces the cancellation of most contributions from $q=0$ excitations.

The first step of these manipulations is to express $\mathscr{E}_{nn'}$ in terms of the eigenvalues $\hat{E}_n$ of the Poisson-Schrödinger equation. We find

$$\mathscr{E}_{nn'} = E_n \delta_{nn'} - \frac{2\pi e^2}{Sa^{-1}} \sum_p \mathscr{N}_p W_{pp;nn'}, \tag{2.13}$$

E_n being related to $\hat{E}_n$ as in Sec. I [Eq. (1.47)].

Next we rewrite the part of $\mathscr{H}_0$ which depends on W as a two-body operator by using the fact that, in the large-N limit, we have

$$\begin{aligned} N A^\dagger_{n\mathbf{k}\sigma} A_{n'\mathbf{k}\sigma} &= \sum_{n_1\mathbf{k}_1\sigma_1} A^\dagger_{n\mathbf{k}\sigma} A_{n'\mathbf{k}\sigma} A^\dagger_{n_1\mathbf{k}_1\sigma_1} A_{n_1\mathbf{k}_1\sigma_1} \\ &\cong \sum_{n_1\mathbf{k}_1\sigma_1} A^\dagger_{n\mathbf{k}\sigma} A^\dagger_{n_1\mathbf{k}_1\sigma_1} A_{n_1\mathbf{k}_1\sigma_1} A_{n'\mathbf{k}\sigma} \end{aligned} \tag{2.14}$$

when this operator acts on any N particle state. This allows us to rewrite the Hartree Hamiltonian as

$$\begin{aligned} \mathscr{H}_H = & \sum_{n\mathbf{k}\sigma} (\varepsilon_k + E_n) A^\dagger_{n\mathbf{k}\sigma} A_{n\mathbf{k}\sigma} \\ & + \frac{1}{2} \frac{2\pi e^2}{Sa^{-1}} \sum_{\substack{n_1 n_1' \\ n_2 n_2'}} \sum_{\substack{\mathbf{k}_1\sigma_1 \\ \mathbf{k}_2\sigma_2}} W'_{n_1n_1';n_2n_2'} A^\dagger_{n_1\mathbf{k}_1\sigma_1} A^\dagger_{n_2\mathbf{k}_2\sigma_2} \\ & \times A_{n_2'\mathbf{k}_2\sigma_2} A_{n_1'\mathbf{k}_1\sigma_1}, \end{aligned} \tag{2.15}$$

where the W' are given by

$$\begin{aligned} W'_{n_1n_1';n_2n_2'} = & W_{n_1n_1';n_2n_2'} - \sum_p \frac{\mathscr{N}_p}{N} [W_{pp;n_2n_2'} \delta_{n_1n_1'} \\ & + W_{n_1n_1';pp} \delta_{n_2n_2'}]. \end{aligned} \tag{2.16}$$

It is easy to check that these W' verify

$$\sum_p \mathscr{N}_p W'_{pp;nn'} = 0 \quad \text{if} \quad n \neq n'. \tag{2.17}$$

The last step is to force such a relation for $n = n'$ as well. For that we add and subtract a constant term NE to $\mathscr{H}_H$ and we write this constant term in two ways:

$$\begin{aligned} NE &= E \sum_{n\mathbf{k}\sigma} A^\dagger_{n\mathbf{k}\sigma} A_{n\mathbf{k}\sigma} \\ &\cong \frac{E}{N} \sum_{n\mathbf{k}\sigma} \sum_{n'\mathbf{k}'\sigma'} A^\dagger_{n\mathbf{k}\sigma} A^\dagger_{n'\mathbf{k}'\sigma'} A_{n'\mathbf{k}'\sigma'} A_{n\mathbf{k}\sigma} \end{aligned} \tag{2.18}$$

according to Eq. (2.14). By choosing

$$\begin{aligned} E &= -\tfrac{1}{2} \int dz\, V_z [\rho_e(z) - \rho_i(z)] \\ &= \pi e^2 n_s \int \int dz\, dz' |z - z'| [\rho_e(z) - \rho_i(z)] \\ &\quad \times [\rho_e(z') - \rho_i(z')] \end{aligned} \tag{2.19}$$

[as in Eq. (1.57)], we transform Eq. (2.15) into Eq. (2.9) and we find that the eigenvalues $\tilde{E}_n$ associated to the diagonal part $\tilde{\mathscr{H}}_0$ are given by

$$\tilde{E}_n = E_n + E = \hat{E}_n + \hat{E} \tag{2.20}$$

with $\hat{E}$ given by Eq. (1.59), while the matrix elements $\tilde{W}_{n_1n_1';n_2n_2'}$ associated to the interaction $\tilde{\mathscr{V}}^{(q=0)}$ are now given by

$$\tilde{W}_{n_1n_1';n_2n_2'} = W'_{n_1n_1';n_2n_2'} + \delta_{n_1n_1'} \delta_{n_2n_2'} \sum_{pp'} \frac{\mathscr{N}_p \mathscr{N}_{p'}}{N^2} W_{pp;p'p'}. \tag{2.21}$$

It is possible to rewrite these $\tilde{W}$ as

$$\begin{aligned} \tilde{W}_{n_1n_1';n_2n_2'} = & - \int \int dz_1\, dz_2 \frac{|z_1 - z_2|}{a} [\phi^*_{n_1}(z_1) \phi_{n_1'}(z_1) \\ & - \rho_e(z_1) \delta_{n_1n_1'}][\phi^*_{n_2}(z_2) \phi_{n_2'}(z_2) - \rho_e(z_2) \delta_{n_2n_2'}]. \end{aligned} \tag{2.22}$$

From the above equation, it is straightforward to check that these $\tilde{W}$ do verify the "magic" equation (2.12). We can also note that $\tilde{W}_{n_1n_1';n_2n_2'}$ looks very much like $W_{n_1n_1';n_2n_2'}$ except that the ion density $\rho_i(z)$ is replaced by the electronic density $\rho_e(z)$.

Up to now, the set of parameters $\mathscr{N}_n$ which enter $\rho_e(z)$ and determine the $|\phi_{n\mathbf{k}}\rangle$ basis are undefined. The last problem is to determine them. Let us do it now.

B. Determination of the $\mathscr{N}_n$ parameters

We consider the state $|\mathscr{N}_1 \cdots \mathscr{N}_n \cdots\rangle$ with $\mathscr{N}_n$ electrons in the lowest $|\phi_{n\mathbf{k}}\rangle$ states of the n subband. $|\mathscr{N}_1 \cdots \mathscr{N}_n \cdots\rangle$ is an eigenstate of $\mathscr{H}_0$ with the energy

$$\mathscr{E}(\mathscr{N}_1 \cdots \mathscr{N}_n \cdots) = \sum_n \mathscr{N}_n \left[\frac{\pi}{2mS} \mathscr{N}_n + \tilde{E}_n \right], \tag{2.23}$$

$\tilde{E}_n$ depending on $\mathscr{N}_n$ through ρ_e. If we now consider the Hamiltonian $\mathscr{H}_H$ and introduce the $\tilde{\mathscr{V}}^{(q=0)}$ interaction as a perturbation, we find that the first-order term of the energy change [corresponding to processes shown in Fig. 3(a)],

$$\begin{aligned} & \langle \mathscr{N}_1 \cdots \mathscr{N}_n \cdots | \tilde{\mathscr{V}}^{(q=0)} | \mathscr{N}_1 \cdots \mathscr{N}_n \cdots \rangle \\ & = \frac{\pi e^2}{Sa^{-1}} \sum_{pp'} \mathscr{N}_p \mathscr{N}_{p'} \tilde{W}_{pp;p'p'} \end{aligned} \tag{2.24}$$

gives zero due to Eq. (2.12). Turning to the second-order term

$$\langle \mathcal{N}_1 \cdots \mathcal{N}_n \cdots | \tilde{\mathcal{V}}^{(q=0)} P_\perp \frac{1}{\mathcal{E} - \tilde{\mathcal{H}}_0} P_\perp \tilde{\mathcal{V}}^{(q=0)} | \mathcal{N}_1 \cdots \mathcal{N}_n \cdots \rangle, \tag{2.25}$$

we find that its extensive contribution also gives zero: The extensive contribution comes from a summation over three arbitrary variables, in order to have a term proportional to the well surface S. It corresponds to the processes shown in Fig. 3(b). Each Coulomb interaction leads to a factor

$$\sum_p \mathcal{N}_p \tilde{W}_{pp;nn'}, \tag{2.26}$$

which is zero due to Eq. (2.12). Similarly, all the higher-order terms also give zero due to the presence of the same factor [Eq. (2.26)]. The apparition of such factors is clearer in the diagrammatic expansion of the energy in powers of $\tilde{\mathcal{V}}^{(q=0)}$, since all terms contain "tadpoles" like the one drawn in Fig. 4.

We thus conclude that the energy of the perturbed state derived from $|\mathcal{N}_1 \cdots \mathcal{N}_n \cdots \rangle$ by applying the $\tilde{\mathcal{V}}^{(q=0)}$ perturbation is simply $\mathcal{E}(\mathcal{N}_1 \cdots \mathcal{N}_n \cdots)$. Consequently, this energy is nothing but the Hartree energy of the $(\mathcal{N}_1 \cdots \mathcal{N}_n \cdots)$ filling.

If we now want to determine the set of $\mathcal{N}_n$ which corresponds to the lowest Hartree energy, we have to minimize $\mathcal{E}(\mathcal{N}_1 \cdots \mathcal{N}_n \cdots)$ with respect to the $\mathcal{N}_n$. As these $\mathcal{N}_n$ are linked by Eq. (2.5), this minimum corresponds to $\mathcal{N}_n = N_n$, with N_n given by

$$\alpha = \left| \frac{\partial E(\mathcal{N}_1 \cdots \mathcal{N}_n \cdots)}{\partial \mathcal{N}_n} \right|_{\mathcal{N}_n = N_n}, \tag{2.27}$$

α being a constant (Lagrange) multiplier. Since $\tilde{E}_n = E_n + E$ and

$$N \frac{\partial E}{\partial \mathcal{N}_n} + \sum_p \mathcal{N}_p \frac{\partial E_p}{\partial \mathcal{N}_n} = 0, \tag{2.28}$$

as shown in Appendix B, Eq. (2.27) reduces to

$$\alpha = \frac{\pi}{mS} N_n + \tilde{E}_n \tag{2.29}$$

in which $\tilde{E}_n$ depends on $N_1 \cdots N_n \cdots$ through ρ_e.

Equation (2.5) (with $\mathcal{N}_n$ replaced by N_n) and Eq. (2.29) are exactly equivalent to Eqs. (1.49) and (1.51), with $\alpha = \mu + E$: The set of $\mathcal{N}_n$ which minimizes the $\mathcal{E}(\mathcal{N}_1 \cdots \mathcal{N}_n \cdots)$ corresponds to the equilibrium filling of the renormalized subbands with localization energies E_n [cf. Fig. 3(c)]. In the particular case of a two-subband filling, we do recover the equilibrium condition [Eq. (1.22)].

We thus conclude that the N_n determined self-consistently from the $T \neq 0$ Green's function formalism of Sec. I are the same as the ones we obtain here using a minimization procedure. Moreover, as can be seen from Eqs. (1.56) and (2.23), $\mathcal{E}(\mathcal{N}_1 \cdots \mathcal{N}_n \cdots)$ is exactly equal to the Hartree energy $\mathcal{E}_H$ calculated in Sec. I. This means that, as we could expect, the $|N_1 \cdots N_n \cdots \rangle$ eigenstate of $\tilde{\mathcal{H}}_0$ is the unperturbed state we have to start from, in order to get the true ground-state energy of the Hartree Hamiltonian.

We wish to end this section with the following remark. Although the introduction of the ρ_e electron density [Eq. (1.4)] would have no physical meaning if not associated to a state with $\mathcal{N}_n$ electrons in the n subband, $\rho_e(z)$ could be considered as a formal parameter which defines the $|\phi_{n\mathbf{k}}\rangle$. We can thus imagine to consider $\tilde{\mathcal{H}}_0$ eigenstates $|\mathcal{N}'_1 \cdots \mathcal{N}'_n \cdots \rangle$ with $\mathcal{N}'_n \neq \mathcal{N}_n$. We do show in Appendix C that the $\mathcal{N}'_n$ and $\mathcal{N}_n$ which give the lowest $\tilde{\mathcal{H}}_0$ eigenenergy are indeed such that $\mathcal{N}'_n = \mathcal{N}_n = N_n$ where N_n still verifies Eq. (2.29).

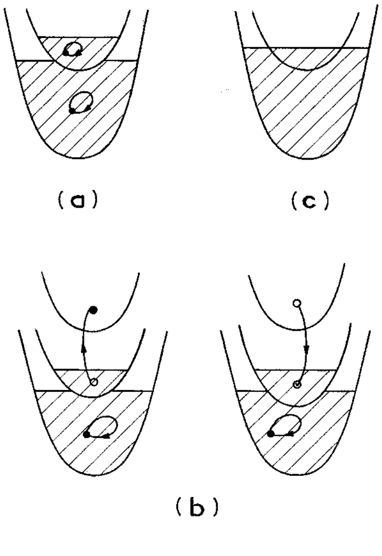

FIG. 3. First-order (a) and second-order (b) excitation processes corresponding to zero momentum transfers (i.e., Hartree interaction). (c) Equilibrium filling for Hartree renormalized subbands.

III. EXCHANGE AND CORRELATION ENERGIES

A. Summary of the basic equations

In the preceding section, we have introduced a Hartree basis $|\phi_{n\mathbf{k}}\rangle = |\phi_n\rangle \otimes |\mathbf{k}\rangle$ in which $|\phi_n\rangle$ is solution of a self-consistent Poisson-Schrödinger equation:

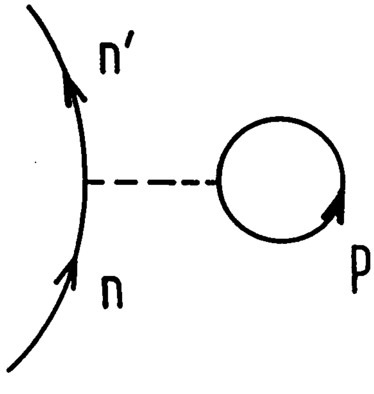

FIG. 4. "Tadpole" diagram appearing in the Hartree expansion.

$$\hat{H}_z|\phi_n\rangle=\hat{E}_n|\phi_n\rangle, \tag{3.1}$$

$$\hat{H}_z=\frac{p_z^2}{2m}+u(z)-2\pi e^2 n_s\int dz'|z-z'|[\rho_e(z')-\rho_i(z')], \tag{3.2}$$

$\rho_e(z)$ being the Hartree electron density given by

$$N\rho_e(z)=\sum_n N_n|\phi_n(z)|^2 \tag{3.3}$$

and N_n the number of electrons in the n subband. These N_n verify

$$\hat{E}_1+\varepsilon_{K_1}=\hat{E}_2+\varepsilon_{K_2}=\cdots \quad \text{with} \quad K_n^2=2\pi N_n/S. \tag{3.4}$$

We have used these Hartree functions as a basis for second quantization, and we have shown that, in terms of the corresponding Hartree creation operators $A^\dagger_{n\mathbf{k}\sigma}$, the total Hamiltonian can be written as

$$\mathcal{H}=\tilde{\mathcal{H}}_0+\tilde{\mathcal{V}}^{(q=0)}+\mathcal{V}^{(q\neq0)}. \tag{3.5}$$

The one-body part $\tilde{\mathcal{H}}_0$ is diagonal and reads

$$\tilde{\mathcal{H}}_0=\sum_{n\mathbf{k}\sigma}(\varepsilon_k+\tilde{E}_n)A^\dagger_{n\mathbf{k}\sigma}A_{n\mathbf{k}\sigma}. \tag{3.6}$$

These $\tilde{E}_n$ differ from the eigenvalues $\hat{E}_n$ of the Poisson-Schrödinger equation by a constant term $\hat{\hat{E}}$, as given in Eq. (1.59).

The two-body part $\tilde{\mathcal{V}}^{(q=0)}$ corresponds to zero-momentum transfer excitations and reads

$$\tilde{\mathcal{V}}^{(q=0)}=\frac{1}{2}\frac{2\pi e^2}{Sa^{-1}}\sum_{\substack{n_1n_1'\\n_2n_2'}}\sum_{\substack{\mathbf{k}_1\sigma_1\\\mathbf{k}_2\sigma_2}}\tilde{W}_{n_1n_1';n_2n_2'}A^\dagger_{n_1\mathbf{k}_1\sigma_1}A^\dagger_{n_2\mathbf{k}_2\sigma_2}\times A_{n_2'\mathbf{k}_2\sigma_2}A_{n_1'\mathbf{k}_1\sigma_1}. \tag{3.7}$$

The main property of the $\tilde{W}$ matrix elements is to verify

$$\sum_p N_p\tilde{W}_{pp;nn'}=0 \quad \forall n,n'. \tag{3.8}$$

They are precisely given by

$$\tilde{W}_{n_1n_1';n_2n_2'}=-\int\int dz_1\,dz_2\frac{|z_1-z_2|}{a}[\phi^*_{n_1}(z_1)\phi_{n_1'}(z_1)-\rho_e(z_1)\delta_{n_1n_1'}][\phi^*_{n_2}(z_2)\phi_{n_2'}(z_2)-\rho_e(z_2)\delta_{n_2n_2'}]. \tag{3.9}$$

The last part, $\mathcal{V}^{(q\neq0)}$, corresponds to Coulomb excitations with nonzero momentum transfer and reads

$$\mathcal{V}^{(q\neq0)}=\frac{1}{2}\sum_{\mathbf{q}\neq0}\frac{2\pi e^2}{Sq}\sum_{\substack{n_1n_1'\\n_2n_2'}}\sum_{\substack{\mathbf{k}_1\sigma_1\\\mathbf{k}_2\sigma_2}}V_{n_1n_1';n_2n_2'}(q)\times A^\dagger_{n_1\mathbf{k}_1+\mathbf{q}\sigma_1}A^\dagger_{n_2\mathbf{k}_2-\mathbf{q}\sigma_2}A_{n_2'\mathbf{k}_2\sigma_2}A_{n_1'\mathbf{k}_1\sigma_1}, \tag{3.10}$$

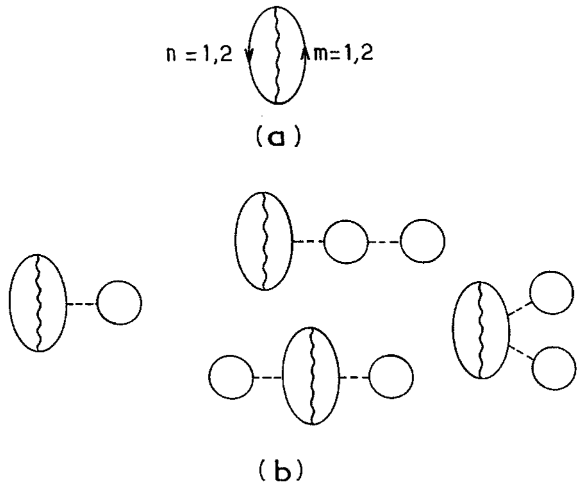

FIG. 5. Exchange energy diagrams (the wavy line corresponds to the $\mathcal{V}^{(q\neq0)}$ interaction): (a) "bare" term, i.e., without Hartree processes; (b) mixed Hartree-exchange terms with one or two $\tilde{\mathcal{V}}^{(q=0)}$ interactions (dashed lines): All these terms give a zero contribution.

$$V_{n_1n_1';n_2n_2'}(q)=\int\int dz_1\,dz_2 e^{-q|z_1-z_2|}\phi^*_{n_1}(z_1)\phi_{n_1'}(z_1)\times\phi^*_{n_2}(z_2)\phi_{n_2'}(z_2). \tag{3.11}$$

The Hartree energy $\mathcal{E}_H$, i.e., the ground-state energy of the Hartree Hamiltonian $\mathcal{H}_H=\tilde{\mathcal{H}}_0+\tilde{\mathcal{V}}^{(q=0)}$, is given by Eq. (1.58). We derived it from two different approaches and showed that it is equal to the unperturbed energy of the $\tilde{\mathcal{H}}_0$ eigenstate $|N_1,N_2,\ldots N_n,\ldots\rangle$.

In this section we will for simplicity restrict our study to a two-subband filling and look for the total Coulomb energy of the perturbed state obtained from the $\tilde{\mathcal{H}}_0$ eigenstate $|N_1N_2\rangle$ when applying the $[\tilde{\mathcal{V}}^{(q=0)}+\mathcal{V}^{(q\neq0)}]$ perturbation. Since $\tilde{\mathcal{V}}^{(q=0)}$ alone gives a zero contribution, as shown in Sec. II, we only have to consider terms with one $\mathcal{V}^{(q\neq0)}$ at least.

B. Exchange energy

The exchange energy contains all terms with one $\mathcal{V}^{(q\neq0)}$, i.e., all terms in $\mathcal{V}^{(q\neq0)}[\tilde{\mathcal{V}}^{(q=0)}]^p$ with $p\geqslant0$. Some of the corresponding diagrams are shown in Fig. 5.

(i) The "bare" exchange energy, i.e., the term without any $\tilde{\mathcal{V}}^{(q=0)}$ Hartree interaction, simply reads

$$\mathcal{E}_x=N\varepsilon_x=\langle N_1N_2|\mathcal{V}^{(q\neq0)}|N_1N_2\rangle=-\sum_{\mathbf{q}\neq0}\frac{2\pi e^2}{Sq}\sum_{\substack{n=1,2\\m=1,2}}V_{nm;mn}(q)J_{nm}(q), \tag{3.12}$$

$$J_{nm}(q)=\sum_{\mathbf{k}}\theta(K_n-k)\theta(K_m-|\mathbf{k}+\mathbf{q}|). \tag{3.13}$$

It corresponds to the diagram of Fig. 5(a) or to the physical processes shown in Fig. 6.

Explicit expressions of $J_{nm}(q)$ are given in Appendix D. From them we can numerically compute the values of ε_x for different values of r_s and a/a_0. They will be given in Sec. IV.

(ii) Turning to the mixed Hartree-exchange energy, i.e., to terms with one or more $\tilde{\mathscr{V}}^{(q=0)}$ interactions [cf. Fig. 5(b)], we find that they all give zero since they all correspond to "tadpole" diagrams [cf. Fig. 4] and thus contain a factor $\Sigma_{p=1,2}N_p\tilde{W}_{pp;nn'}$ which is zero due to Eq. (3.8).

Within our renormalized Hartree approach, we thus conclude that the exchange energy reduces to its "bare" value $\mathscr{E}_x$ only, as given in Eq. (3.12). Let us stress that this "bare" value is not really a bare value since it contains some Hartree effects through the Hartree wave functions $\phi_n(z)$ entering the Coulomb matrix element $V_{nm;mn}(q)$.

C. Correlation energy

The correlation energy contains all terms in $(\mathscr{V}^{(q\neq 0)})^l(\tilde{\mathscr{V}}^{(q=0)})^p$ with $l\geqslant 2$ and $p\geqslant 0$. We will only discuss here the second-order terms, i.e., the terms with $l=2$.

(i) The "bare" second-order correlation term has no $\tilde{\mathscr{V}}^{(q=0)}$ interaction. It is given by

$$\mathscr{E}^{(2)}_{\text{corr}}=\sum_{|n\rangle\neq|N_1,N_2\rangle}\frac{|\langle n|\mathscr{V}^{(q\neq 0)}|N_1N_2\rangle|^2}{E(N_1,N_2)-E(n)}. \tag{3.14}$$

$\mathscr{E}^{(2)}_{\text{corr}}$ contains the usual direct and exchange terms as well as an "anomalous" term. These contributions correspond to the diagrams of Fig. 7(a). The direct and exchange terms read

$$\mathscr{E}^{d+e}_{\text{corr}}=\left(\frac{2\pi e^2}{S}\right)\sum_{\substack{n_1=1,2\\ n_2=1,2}}\sum_{\mathbf{q}\neq 0}\sum_{\substack{n_1'n_2'\\ \mathbf{k}_1\mathbf{k}_2}}\frac{f_{n_1\mathbf{k}_1}(1-f_{n_1',\mathbf{k}_1+\mathbf{q}})f_{n_2\mathbf{k}_2}(1-f_{n_2',\mathbf{k}_2-\mathbf{q}})}{\hat{E}_{n_1}+\hat{E}_{n_2}-\hat{E}_{n_1'}-\hat{E}_{n_2'}+\varepsilon_{k_1}+\varepsilon_{k_2}-\varepsilon_{\mathbf{k}_1+\mathbf{q}}-\varepsilon_{\mathbf{k}_2-\mathbf{q}}}$$
$$\times\left[\frac{2|V_{n_1n_1';n_2n_2'}(q)|^2}{q^2}-\frac{V_{n_1n_1';n_2n_2'}(q)V_{n_1'n_1;n_2'n_2}(|\mathbf{q}+\mathbf{k}_1-\mathbf{k}_2|)}{q|\mathbf{q}+\mathbf{k}_1-\mathbf{k}_2|}\right] \tag{3.15}$$

[where $f_{n\mathbf{k}}$ is the Fermi function $f_{n\mathbf{k}}=\theta(K_n-|\mathbf{k}|)$], while the anomalous term is given by

$$\mathscr{E}^{a}_{\text{corr}}=2\left(\frac{2\pi e^2}{S}\right)^2\sum_{\substack{n_1=1,2\\ n_2=1,2\\ n_3=1,2}}\sum_{\substack{n_3'\neq n_3\\ \mathbf{k}_1\mathbf{k}_2\mathbf{k}_3}}\frac{f_{n_1\mathbf{k}_1}f_{n_2\mathbf{k}_2}f_{n_3\mathbf{k}_3}(1-f_{n_3'\mathbf{k}_3})}{\hat{E}_{n_3}-\hat{E}_{n_3'}}$$
$$\times\frac{V_{n_1n_3;n_3'n_1}(|\mathbf{k}_3-\mathbf{k}_1|)V_{n_3n_2;n_2n_3'}(|\mathbf{k}_3-\mathbf{k}_2|)}{|\mathbf{k}_3-\mathbf{k}_1||\mathbf{k}_3-\mathbf{k}_2|}. \tag{3.16}$$

Equations (3.15) and (3.16) are formally similar to Eqs. (7) and (8) of Ref. 2 except that the subband indices n_1,n_2,n_3 can here be equal to 1 or 2 (and not to 1 only) due to the fact that electrons now occupy two subbands.

Let us stress that, here again, this "bare" second-order energy is not really bare since the Hartree effects are present

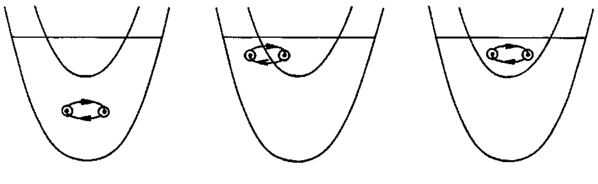

FIG. 6. Exchange processes of the "bare" term inside the $n=1$ subband, inside the $n=2$ subband, and between the $n=1$ and $n=2$ subbands.

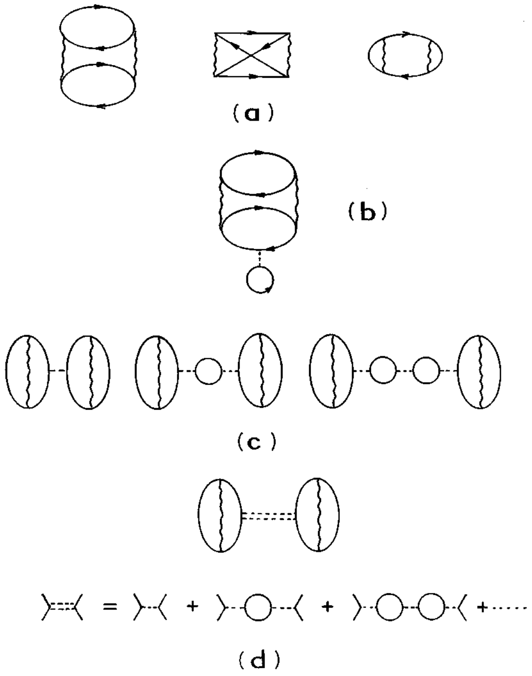

FIG. 7. (a) "Bare" second-order correlation diagrams. The third diagram, called the "anomalous" diagram, does not exist in the 3D and exact 2D expansions at $T=0$: It comes from possible intersubband excitations only. (b) One possible mixed Hartree-second-order correlation diagram; such diagrams are generated by adding a "tadpole" to the "bare" diagrams of (a): All these terms give a zero contribution. (c) Other mixed Hartree-second-order correlation diagrams, which are not obtained by simply adding a "tadpole" to the "bare" correlation diagrams. (d) Summation of all the diagrams of the type shown in (c).

through the $\hat{E}_n$ and the $V_{n_1 n_1' ; n_2 n_2'}(q)$, which depend on the ϕ_n. This makes the numerical calculation of the correlation energy rather heavy when compared to the one of Ref. 2: Indeed, in the perturbative treatment of the Hartree processes, we used the free-electron basis $\varphi_{n\mathbf{k}}$ which is known analytically for infinite well barriers. This allowed an analytical calculation of all $V_{n_1 n_1' ; n_2 n_2'}$ matrix elements, so that only the last sums entering the correlation energy had to be calculated numerically. On the contrary, for these correlation terms, we have here to numerically compute *all* the ϕ_n functions in a self-consistent way, using Eqs. (3.1) and (3.2), then calculate all $V_{n_1 n_1' ; n_2 n_2'}(q)$ matrix elements with one or two subbands indices equal to any integer value (the other indices being equal to 1 or 2), and eventually compute the sums entering the correlation energy. As the ϕ_n wave functions depend on the precise ion configuration, such heavy numerical work appears to us useless unless we can compare the results with experimental ones. [Let us note that the exchange energy is much easier to get since it contains the $V_{n_1 n_1' ; n_2 n_2'}(q)$ matrix elements with subband indices equal to 1 or 2 only, so that only ϕ_1 and ϕ_2 have to be determined self-consistently.]

(ii) If we now turn to the mixed Hartree-correlation energy, we can first think of adding $\tilde{\mathscr{V}}^{(q=0)}$ processes to the three diagrams corresponding to $\mathscr{E}_{\rm corr}^{(2)}$. We get diagrams like the one of Fig. 7(b). In all of them $\tilde{\mathscr{V}}^{(q=0)}$ Hartree processes are associated to "tadpoles," so that their contributions give zero due again to Eq. (3.8).

(iii) However, we should not hastily conclude that no $\tilde{\mathscr{V}}^{(q=0)}$ contribution enters the second-order correlation energy. Indeed, there are other diagrams with $\tilde{\mathscr{V}}^{(q=0)}$ processes which differ from "tadpoles," as can be seen from Fig. 7(c). The sum of such diagrams can be formally written in terms of a renormalized interaction $\hat{W}_{n_1 n_1' ; n_2 n_2'}$ shown in Fig. 7(d) and given by

$$\hat{W}_{n_1 n_1' ; n_2 n_2'} = \tilde{W}_{n_1 n_1' ; n_2 n_2'} + \sum_{n_3 \neq n_3'} \tilde{W}_{n_1 n_1' ; n_3 n_3'} \Pi_{n_3 n_3'} \tilde{W}_{n_3' n_3 ; n_2 n_2'} + \sum_{\substack{n_3 \neq n_3' \\ n_4 \neq n_4'}} \tilde{W}_{n_1 n_1' ; n_3 n_3'} \Pi_{n_3 n_3'} \tilde{W}_{n_3' n_3 ; n_4 n_4'} \Pi_{n_4 n_4'} \tilde{W}_{n_4' n_4 ; n_2 n_2'} + \cdots$$

$$= \tilde{W}_{n_1 n_1' ; n_2 n_2'} + \sum_{n_3 \neq n_3'} \tilde{W}_{n_1 n_1' ; n_3 n_3'} \Pi_{n_3 n_3'} \hat{W}_{n_3' n_3 ; n_2 n_2'}, \tag{3.17}$$

with

$$\Pi_{nn'} = \frac{2\pi e^2}{S a^{-1}} \frac{N_n - N_{n'}}{\hat{E}_n - \hat{E}_{n'}}, \tag{3.18}$$

the filling N_n of the n subband being the equilibrium filling (in particular $N_n = 0$ for $n \neq 1,2$). Unfortunately it is not possible to find an analytical solution to this implicit equation for the renormalized interaction $\hat{W}_{n_1 n_1' ; n_2 n_2'}$.

We could at first find it useful to note that the set of diagrams shown in Fig. 7(d) correspond to processes included in the self-consistent Hartree-Fock equations. Consequently they can be summed up when added to other mixed $\mathscr{V}^{(q\neq 0)} \tilde{\mathscr{V}}^{(q=0)}$ processes. Besides the numerical complexity of solving these Hartree-Fock equations, we must stress the inconsistency of such a procedure, since it includes additional crossed processes on the behalf that they help for a summation, while it discards other correlation terms of the same order in r_s.

IV. NUMERICAL RESULTS

We now report some numerical results obtained from the self-consistent treatment of Hartree processes in quantum wells which has been developed above. Since these Hartree processes are physically related to the charge separation, they depend on the precise ion configuration. As previously shown within a perturbative treatment of the Hartree interaction,[2] the effect of Hartree processes is larger for ions outside the well than for ions inside. We will concentrate here on this "outside" situation and consider a quantum well with electrons located at $0 < z < a$ and ions located symmetrically on both sides of the well, with

$$\rho_i(z) = \frac{1}{a} \quad \text{for} \quad -\frac{a}{2} < z < 0 \quad \text{and} \quad a < z < \frac{3a}{2}. \tag{4.1}$$

We must stress that the results given below are valid for this choice of $\rho_i(z)$ only: for another ion configuration, all numerical calculations should be performed again.

As discussed in Sec. I, a self-consistent treatment of the Hartree processes is necessary for $\lambda_H > 1$ only, while a reliable treatment of the exchange-correlation effects imposes $r_s < 1$. As shown in Fig. 1, this corresponds to electrons in more than one subband. For the sake of simplicity, we will illustrate our self-consistent approach in the case of a two-subband filling only. The corresponding results will be given for two different values of the well width ($a/a_0 = 1$ and $a/a_0 = 3$). The larger the width, the larger the λ_H parameter and thus the larger the Hartree effects.

A. Subband fillings

Let us first introduce as a particle number unit, the particle number N_0 associated to the lowest binding energy (in the absence of Coulomb interaction), ε_1, through the relation

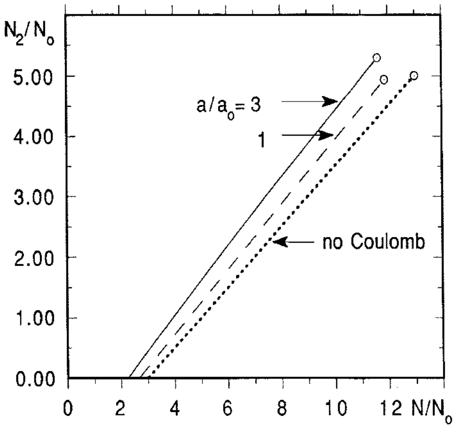

FIG. 8. Number N_2 of electrons in the $n=2$ subband as a function of the total number N of electrons, in N_0 units [defined in Eq. (4.2)]. The threshold for a two-subband filling is pushed from $N/N_0=3$ towards a lower value by the Hartree interaction. This effect increases with the well width a. The open dots correspond to the threshold for a three-subband filling.

$$\varepsilon_1=\frac{1}{2m}\frac{\pi^2}{a^2}=\frac{1}{2m}\frac{2\pi N_0}{S}. \tag{4.2}$$

The ratio N/N_0 is proportional to the 2D electron density n_s and to the square of the well width a:

$$\frac{N}{N_0}=\frac{2}{\pi}n_s a^2. \tag{4.3}$$

In the absence of a Coulomb interaction, the two-subband filling condition given by Eq. (1.19) reads

$$3<N/N_0<13. \tag{4.4}$$

Hartree processes modify this condition, according to Eq. (1.52). As can be seen from Fig. 8, which gives the number N_2 of electrons in the $n=2$ subband as a function of the total particle number N, the electrons begin to fill the $n=2$ subband for $N/N_0<3$: The two-subband filling occurs as soon as $N/N_0=2.68$ for $a/a_0=1$, and $N/N_0=2.25$ for $a/a_0=3$. As expected, the effect is stronger for $a/a_0=3$ than for $a/a_0=1$.

In the absence of Hartree interaction, the N_2 versus N curve is exactly linear with a slope equal to 0.5 (the average kinetic energy of electrons in a given subband being in 2D proportional to the number of electrons in this subband). We see that Hartree processes do not modify very much this behavior: the N_2 versus N curve is almost linear with a slope slightly larger than 0.5. This occurs from the fact that the (E_2-E_1) energy difference between the bottoms of the $n=1$ and $n=2$ subbands decreases slightly with N, as shown below.

Hartree processes also modify the value of N/N_0 for which the $n=3$ subband begins to be filled. This threshold reduces from 13 to 11.88 for $a/a_0=1$ and 11.62 for $a/a_0=3$.

Let us stress that, although N_0 may appear as an appropriate particle number unit, it depends on the well width [see Eqs. (4.2) and (4.3)]. Consequently, plots in N_0 units can only give a partial view of the well-width effect on the subband filling. This is why we have also plotted in Fig. 9 the fraction N_2/N of electrons in the $n=2$ subband as a function of r_s^{-1} (which is proportional to $\sqrt{n_s}a_0$), the dotted curves corresponding to the results in the absence of Hartree effects. As expected, we find that the smaller the well width, the larger the density necessary to have electrons in the $n=2$ subband (the subband separation being infinite for zero well width). Here again we note that the Hartree processes give a larger effect for larger a.

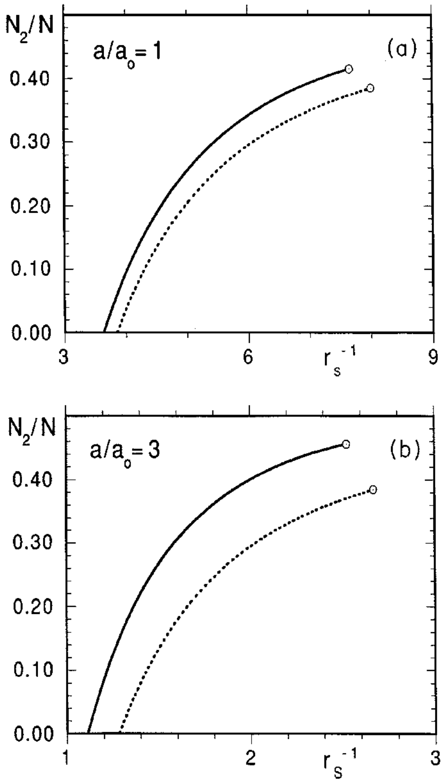

FIG. 9. Fraction of electrons in the $n=2$ subband as a function of $(r_s)^{-1}$, for two well widths: $a/a_0=1$ (a) and $a/a_0=3$ (b). The dotted curves correspond to the results in the absence of Hartree effects and the open dots correspond to the threshold for a three-subband filling.

B. Hartree renormalized subband energies

In Fig. 10 we report the energy differences between the $n=1,2,3$ subband bottoms, in the presence of Hartree interaction, as a function of N/N_0 for two different well widths. Due to Eq. (2.20), these differences are also the differences between the Poisson-Schrödinger eigenenergies $\hat{E}_1,\hat{E}_2,\hat{E}_3$.

In the absence of Coulomb interaction, these differences are simply $E_2-E_1=3\varepsilon_1$ and $E_3-E_2=5\varepsilon_1$. Hartree effects induce a density dependence which increases with the well width. We see a break point at the two-subband filling threshold (as indicated by arrows). The difference (E_2-E_1) monotonously decreases with N/N_0, in agreement with the increase of the slope of the N_2 versus N curve shown in Fig. 8. The difference (E_3-E_2) is much less modified than (E_2-E_1); it slightly decreases for $a/a_0=1$ while it shows a minimum in the vicinity of the two-subband filling threshold for $a/a_0=3$.

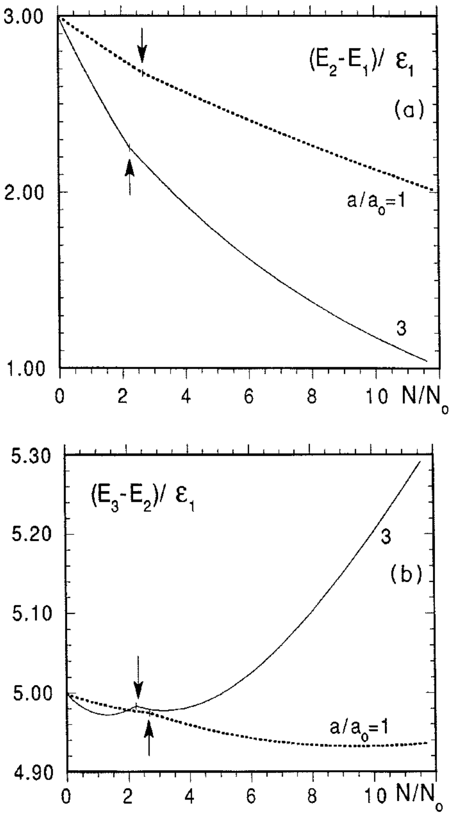

FIG. 10. Energy differences between the $n=1$ and $n=2$ subbands (a) and between the $n=2$ and $n=3$ subbands (b), when renormalized by the Hartree interaction, for two well widths, as a function of the electron number N. In the absence of Hartree effects, these differences are $3\varepsilon_1$ and $5\varepsilon_1$ (ε_1 being the lowest binding energy of the well). The arrows indicate the threshold for a two-subband filling.

C. Hartree wave functions

Other interesting "one-particle" quantities are the electron wave functions: Fig. 11 shows the square of the Hartree wave functions $|\phi_n(z)|^2$ for $n=1$, 2, and 3 in the case of the larger well width $a/a_0=3$, and for an electron number $N/N_0=8$. In this case the fillings are $N_1/N_0\cong 4.7$, $N_2/N_0\cong 3.3$. The free-electron square wave functions $|\varphi_n(z)|^2$ are drawn as dotted curves for comparison. From them we can appreciate the effect of the Hartree interaction.

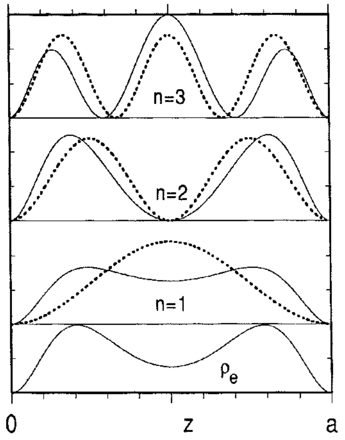

FIG. 11. Squares of the Hartree renormalized wave functions of the $n=1$, $n=2$, $n=3$ subbands for $a/a_0=3$ and $N/N_0=8$ (in this case $N_2/N_0=3.3$ and $N_3=0$). The corresponding electronic charge density $\rho_e(z)$ is also shown. The dotted curves correspond to the same wave functions in the absence of Hartree effects.

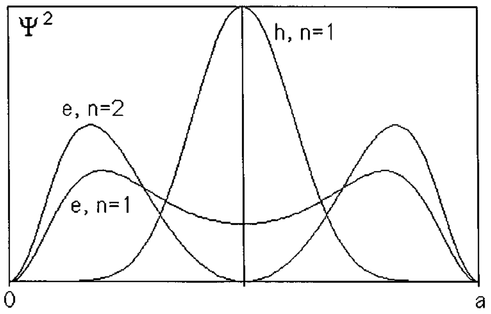

FIG. 12. Square of the Hartree renormalized wave function of the $n=1$ hole subband for $a/a_0=3$ and $N/N_0=11.6$. The squares of the corresponding electron $n=1$ and $n=2$ wave functions are also shown.

Figure 11 also shows the electronic charge density $\rho_e(z)$ as given by Eq. (3.3). To that density corresponds an electrostatic potential V with a maximum at the well center. This maximum affects strongly the $n=1$ wave function which is depressed at the center. Modifications of the $n=2$ and $n=3$ wave functions are smaller because E_2 and E_3 are larger with respect to V. The fact that the central part of the $n=3$ wave function increases when compared with the free electron one may be understood by the requirement of orthogonality with the $n=1$ wave function.

D. Electron-hole Hartree chemical potential

The Hartree chemical potential μ introduced in the finite-temperature approach of Sec. I is the energy necessary to add one electron and one ion to the N electron-ion system in the presence of the Hartree interaction. As this quantity is not easy to measure experimentally, it appears interesting to calculate another chemical potential, namely, the electron-hole chemical potential which is the energy necessary to add one electron and one hole to the same N electron-ion system. This last potential is directly linked to the photon energy threshold of a doped quantum well.

In order to obtain this electron-hole chemical potential, we first have to find the binding energy of the hole in the presence of the Hartree potential of N electrons and ions, i.e., to solve the Poisson-Schrödinger equation for the hole, namely,

$$\hat{H}_z^h|\phi_n^h\rangle=\hat{E}_n^h|\phi_n^h\rangle,$$

$$\hat{H}_z^h=\frac{p_z^2}{2m_h}+u(z)+2\pi e^2 n_s\int dz'|z-z'|[\rho_e(z')-\rho_i(z')]. \tag{4.5}$$

Equation (4.5) is the analogous to Eq. (1.46) with the electron mass m replaced by the hole mass m_h and e^2 changed into $-e^2$.

Figure 12 shows the hole Hartree wave function of the

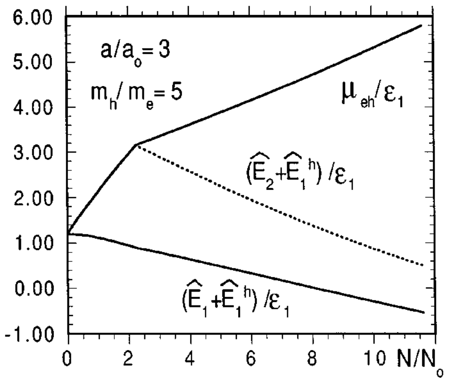

FIG. 13. The lowest solid curve gives $\hat{E}_1+\hat{E}_1^h$, i.e., the sum of the Hartree renormalized energies of the $n=1$ electron and $n=1$ hole subbands, for $a/a_0=3$. The dashed curve gives $\hat{E}_2+\hat{E}_1^h$, where $\hat{E}_2$ is the Hartree renormalized energy of the $n=2$ electron subband. The upper solid curve gives the electron-hole chemical potential μ_{eh} as a function of N; the slope change occurs at the electron two-subband filling threshold, i.e., for $N/N_0 \cong 2.25$. The zero of energy is taken at the band gap.

$n=1$ subband for $N/N_0=11.6$, $a/a_0=3$, and $m_h/m=5$. We have also shown the electron Hartree wave functions of the filled subbands, $n=1$ and $n=2$.

In Fig. 13, we have plotted the sums $(\hat{E}_1+\hat{E}_1^h)$ and $(\hat{E}_2+\hat{E}_1^h)$ in ε_1 unit as functions of N/N_0 (the last sum is reported in the two-subband filling range only, i.e., for $N/N_0 \geqslant 2.2$ if $a/a_0=3$). The electron-hole potential μ_{eh} is given by

$$\mu_{eh}^{(1)}=\hat{E}_1+\hat{E}_1^h+\frac{K^2}{2m}, \quad K^2=\frac{2\pi}{S}N \tag{4.6}$$

in the one-subband filling region, and by

$$\mu_{eh}^{(2)}=\hat{E}_2+\hat{E}_1^h+\frac{K_1^2}{2m}+\frac{K_2^2}{2m}, \quad K_i^2=\frac{2\pi}{S}N_i \tag{4.7}$$

in the two-subband filling region. It is plotted in the same figure.

Of course, in order to obtain the true threshold for photon absorption, we should add to μ_{eh} the band gap and possibly the hole kinetic energy necessary to insure the momentum conservation of a direct absorption. Let us note that the $\hat{E}_1+\hat{E}_1^h$ curve also gives the $T=0$ low-level luminescence, if we assume momentum conservation in the luminescence process.

E. Average Hartree energy

Let us now turn to the Hartree energy $\mathscr{E}_H$ of the N electrons and ions, as given by Eqs. (1.56) or (1.58). In order to have an idea of the energy change induced by the Hartree processes we must subtract from it the energy of N free electrons in the well, namely,

$$\mathscr{E}^{(0)}=\frac{\pi}{2mS}\sum_n (N_n^0)^2+\sum_n N_n^0\varepsilon_n, \tag{4.8}$$

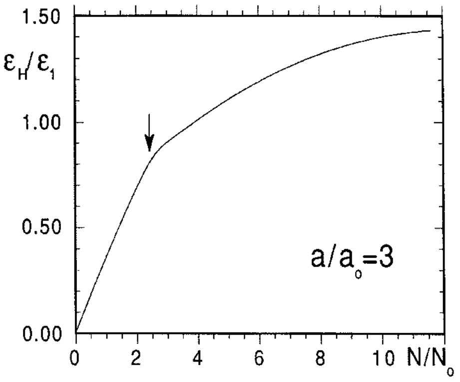

FIG. 14. Average Hartree energy ε_H as a function of the electron number N, for $a/a_0=3$. The arrow indicates the two-subband filling threshold. The units ε_1 and N_0 both depend on the well width.

N_n^0 being given by Eq. (1.18). The difference $(\mathscr{E}_H-\mathscr{E}^{(0)})$ is expected to be dominated by a trivial electrostatic term $N\varepsilon_S$ coming from the energy necessary to separate the electrons from the ions. Following Ref. 1 we define it as

$$\varepsilon_S=\pi n_s e^2 a v,$$

$$v=-\int\int dz_1 dz_2 \frac{|z_1-z_2|}{a}[\bar{\rho}_e(z_1)-\rho_i(z_1)] \times[\bar{\rho}_e(z_2)-\rho_i(z_2)], \tag{4.9}$$

$\bar{\rho}_e(z)$ being the density of electrons delocalized in a negative jellium inside the well $[\bar{\rho}_e(z)=1/a$ for $0<z<a]$. $N\varepsilon_S$ is just the energy necessary to create the charge distribution $n_s e[\rho_i(z)-\bar{\rho}_e(z)]$. The remaining energy

$$\mathscr{E}_H-\mathscr{E}^{(0)}-N\varepsilon_s=N\varepsilon_H \tag{4.10}$$

comes from the subtle changes of the electron wave functions due to the Hartree processes, these changes inducing both a change in the well binding energies and a change in the subband fillings.

In Fig. 14, we have plotted ε_H in ε_1 unit, as a function of N/N_0 for $a/a_0=3$. The arrow indicates the two-subband filling threshold. Here again we see a break point at this threshold. We can also note that in the whole density range corresponding to a two-subband filling, ε_H is of the order of ε_1.

In Fig. 15, we show the same energy ε_H, expressed in Rydberg unit, as a function of $r_s^{-1}\sim\sqrt{n_s a_0^2}$, for a further comparison with the average exchange energy.

F. Exchange energy

We know that in the exact 2D limit, i.e., for $a=0$, the average exchange energy in R_0 unit is simply given by

$$\frac{\mathscr{E}_x^{(00)}}{NR_0}=\frac{\varepsilon_x^{(00)}}{R_0}=-\frac{1{,}20}{r_s}. \tag{4.11}$$

(a) If we include the finite well width *without taking into account Hartree processes,* we have shown[2] that the average exchange energy depends on the well width through a unique parameter λ defined as

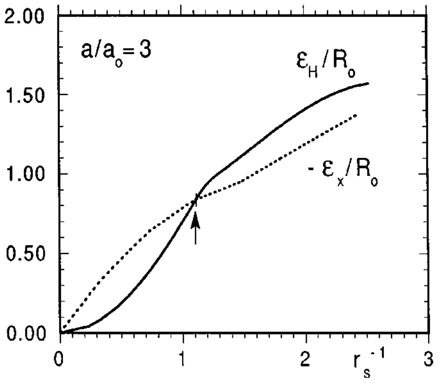

FIG. 15. Average Hartree energy ε_H, in R_0 unit, as a function of $(r_s)^{-1}$, i.e., the same result as the one shown in Fig. 14, using units independent of the well width. The dotted curve, which corresponds to the exchange energy, is given for comparison.

$$\lambda=\frac{Ka}{2\pi}=\frac{1}{2}\left(\frac{N}{N_0}\right)^{1/2} \tag{4.12}$$

and can be written in the form

$$\frac{\varepsilon_x^{(0)}}{R_0}=-\frac{A_x(\lambda)}{r_s} \tag{4.13}$$

[see Eq. (4) of Ref. 2]. Figure 16 shows $A_x(\lambda)$ in the one-subband filling range $(0<\lambda<\sqrt{3}/2)$, as already given in Ref. 2. We also show it in the two-subband filling range, this $A_x(\lambda)$ being simply obtained from Eq. (3.12) with K_n replaced by K_n^0 defined by Eq. (1.18) and $V_{nm;mn}(q)$ replaced by $v_{nm;mn}(q)$ defined by Eq. (1.12). We see that this exchange energy decreases with the well width, with again a break point at the two-subband filling threshold (indicated by an arrow).

(b) If we now include the Hartree processes in a self-consistent way, as done in Sec. III, all mixed Hartree-exchange terms give zero and only the "bare" exchange term given by Eq. (3.12) remains. We can plot this exchange energy in various ways.

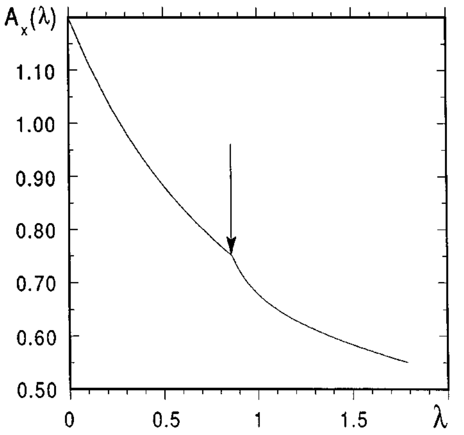

FIG. 16. Average exchange energy [multiplied by $(-r_s)$], in the absence of Hartree processes, as a function of $\lambda=Ka/2\pi$. The arrow indicates the two-subband filling threshold.

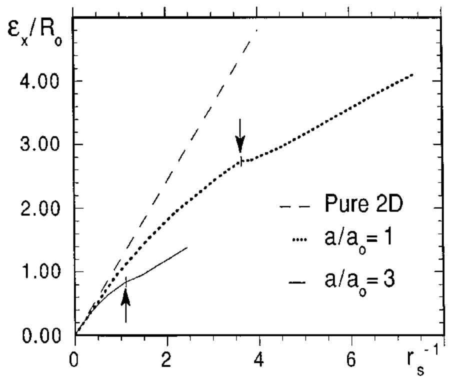

FIG. 17. Average exchange energy in the presence of Hartree processes as a function of $(r_s)^{-1}$, for two well widths. The dashed line corresponds to the exact 2D limit.

In Fig. 17 we show the average exchange energy ε_x in R_0 unit as a function of r_s^{-1}, for $a/a_0=1$ and $a.a_0=3$. We have also plotted the exact 2D limit [Eq. (4.11)] for comparison. The arrow indicates the two-subband filling threshold. (Note that the validity of our exchange-correlation energy calculation implies $r_s<1$ so that the results for $0<r_s^{-1}<1$ are meaningless and are just indicated to guide the eyes.)

The same ε_x/R_0 versus r_s^{-1} curve for $a/a_0=3$ is also plotted in Fig. 15, in order to allow a direct comparison of the exchange energy with the nontrivial part of the average Hartree energy ε_H given by Eq. (4.10). We see that, with our choice of ε_s for the electrostatic part, the average exchange energy ε_s just compensates ε_H at the two-subband filling threshold, but this is accidental.

In order to measure the effect of the self-consistent treatment of the Hartree processes on the exchange energy, we can rewrite ε_x as

$$\frac{\varepsilon_x}{R_0}=-\frac{A_x(\lambda,a/a_0)}{r_s} \tag{4.14}$$

and compare $A_x(\lambda,a/a_0)$ with $A_x(\lambda)$, defined by Eq. (4.13). As $A_x(\lambda)$ gives the exchange energy in the absence of Hartree processes, we do have $A_x(\lambda)\equiv A_x(\lambda,0)$. In Fig. 18, we show $A_x(\lambda,a/a_0)$ for $a/a_0=1$ and $a/a_0=3$ as well as $A_x(\lambda)$. We see that all the curves are very close to each other, which means that Hartree effects on the exchange energy are rather small. The larger effect appears in the vicinity of the two-subband filling threshold and even in this case, it is not larger than 10%. We thus conclude that in most cases we could avoid the self-consistent treatment of the Hartree processes contributing to the exchange energy and simply replace $A_x(\lambda,a/a_0)$ by $A_x(\lambda)$ shown in Fig. 16.

In Fig. 18, we have also plotted the 3D limit of the exchange energy

$$\frac{\varepsilon_x^{(3D)}}{R_0}=-\frac{0.916}{r_s^{(3D)}}=-\frac{0.613}{r_s}\lambda^{-1/3}. \tag{4.15}$$

It is interesting to note that, in the two-subband filling region, the exchange energy is closer to the 3D limit value (roughly 10% above this 3D value) than to the 2D limit value (roughly one-half of this 2D value), even though the 3D limit should correspond to an infinite number of filled subbands.

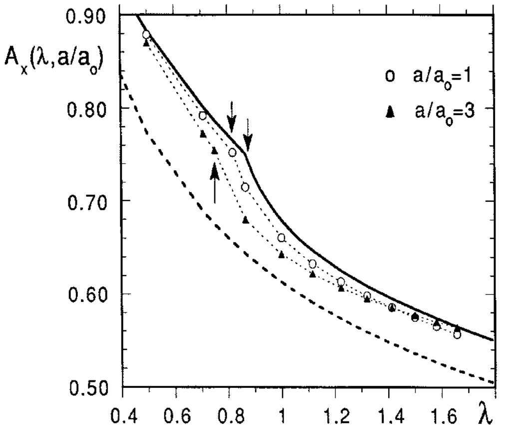

FIG. 18. Same results as those shown in Fig. 17, with $\varepsilon_x/R_0=-(r_s)^{-1}A_x\ (\lambda,a/a_0)$, plotted as functions of λ. The solid curve corresponds to the exchange energy in the absence of Hartree effects (cf. Fig. 16). We see that all these curves are rather close to each other. The dashed curve which corresponds to the 3D limit is also surprisingly close to the other ones, in the two-subband filling region.

V. CONCLUSION

In this paper, we consider an electron gas confined in a finite-width quantum well, dense enough to have electrons in more than one subband. This situation is particularly complex for two reasons: (i) the Hartree processes cannot be treated in a perturbative way as in our previous works; (ii) the Coulomb interaction affects the number of electrons in each subband.

We have developed an approach based on the introduction of Hartree creation operators associated to the self-consistent solutions of the usual Poisson-Schrödinger equation. This allows us to rewrite the total Hamiltonian of the system as a one-body part $\tilde{\mathscr{H}}_0$ plus two two-body parts $\tilde{\mathscr{V}}^{(q=0)}$ and $\mathscr{V}^{(q\neq 0)}$ in such a way that most of the $\tilde{\mathscr{V}}^{(q=0)}$ contributions to the energy cancel. It is indeed impossible to find a transformation which makes all $q=0$ processes disappear: A few mixed $(q=0,q\neq 0)$ contributions do remain in the correlation energy which have to be added to the usual terms.

We give numerical results for the exchange energy (i.e., the first-order term in $\mathscr{V}^{(q\neq 0)}$) in the case of ions on both sides of the well, for which the Hartree processes could be expected to give a rather large effect. It turns out that, in the whole two-subband-filling domain, the exchange energy stays quite close to its bare value, as calculated without any Hartree effect. This result is of practical interest since it allows us to obtain a fairly good value of the exchange energy from a universal one-parameter curve for all ion configurations and well widths.

APPENDIX A: EXPRESSION OF THE HARTREE SELF-ENERGY IN TERMS OF THE HARTREE POTENTIAL:

Inserting Eq. (1.41) into Eqs. (1.25) and (1.26) we get

$$\sigma_{nn'}=\frac{2\pi e^2}{Sa^{-1}}\sum_{\substack{n_1n_2\\n''}} w_{nn';n_1n_2}\langle\varphi_{n_2}|\phi_{n''}\rangle\langle\phi_{n''}|\varphi_{n_1}\rangle N_{n''}, \tag{A1}$$

where we have set

$$N_n=\lim_{\tau\to 0^+} T\sum_{\nu\mathbf{k}\sigma} e^{i\omega_\nu\tau}G_n(k,\omega_\nu). \tag{A2}$$

Since the trace of a matrix does not depend on the basis, we have

$$\sum_n N_n=\sum_n \mathscr{N}_{nn}=\bar{N}(\mu,T)=N. \tag{A3}$$

Inserting the w definition [Eq. (1.10)] into Eq. (A1) we get

$$\begin{aligned}\sigma_{nn'}=&-\frac{2\pi e^2}{S}\int\int dz_1\ dz_2|z_1-z_2|[\varphi_n^*(z_1)\varphi_{n'}(z_1)-\rho_i(z_1)\delta_{nn'}]\sum_{n_1n_2n''}[\langle\varphi_{n_1}|z_2\rangle\langle z_2|\varphi_{n_2}\rangle\langle\varphi_{n_2}|\phi_{n''}\rangle\\&\times\langle\phi_{n''}|\varphi_{n_1}\rangle N_{n''}-\delta_{n_1n_2}\rho_i(z_2)\langle\varphi_{n_2}|\phi_{n''}\rangle\langle\phi_{n''}|\varphi_{n_1}\rangle N_{n''}]\\=&-\frac{2\pi e^2}{S}\int\int dz_1\ dz_2|z_1-z_2|[\varphi_n^*(z_1)\varphi_{n'}(z_1)-\rho_i(z_1)\delta_{nn'}]\left[\sum_{n''}N_{n''}|\phi_{n''}(z_2)|^2-N\rho_i(z_2)\right].\end{aligned} \tag{A4}$$

From the expression of the average electron density $\bar{n}(z,\mu,T)$ [Eq. (1.29)], we find, using Eqs. (1.41) and (A2),

$$\bar{n}(z,\mu,T)=\sum_n N_n|\phi_n(z)|^2.$$

By setting

$$\rho_e(z)=\frac{1}{N}\bar{n}(z,\mu,T), \tag{A5}$$

$$V_z=-2\pi e^2n_s\int dz'|z-z'|[\rho_e(z')-\rho_i(z')], \tag{A6}$$

we see that $\sigma_{nn'}$ reads

$$\sigma_{nn'}=\int dz_1\ \varphi_n^*(z_1)\varphi_{n'}(z_1)V_{z_1}-\delta_{nn'}\int dz_1\rho_i(z_1)V_{z_1}. \tag{A7}$$

The σ_z self-energy is thus related to the V_z Hartree potential through

$$\sigma_z = V_z - \int dz\ V_z \rho_i(z). \tag{A8}$$

APPENDIX B: DERIVATION OF EQ. (2.28)

From Eqs. (2.3) and (1.47) we obtain

$$\begin{aligned}\frac{\partial E_p}{\partial \mathcal{N}_n} &= \frac{\partial}{\partial \mathcal{N}_n}\left\{\int dz\ \phi_p^*(z)[h_z + V_z]\phi_p(z) \right.\\ &\qquad \left. - \int dz\ V_z \rho_i(z)\right\}\\ &= E_p \int dz\left[\frac{\partial \phi_p^*(z)}{\partial \mathcal{N}_n}\phi_p(z) + \phi_p^*(z)\frac{\partial \phi_p(z)}{\partial \mathcal{N}_n}\right]\\ &\quad + \int dz[|\phi_p(z)|^2 - \rho_i(z)]\frac{\partial V_z}{\partial \mathcal{N}_n}\\ &= \int dz[|\phi_p(z)|^2 - \rho_i(z)]\frac{\partial V_z}{\partial \mathcal{N}_n}\end{aligned} \tag{B1}$$

[since $\int dz|\phi_p(z)|^2 = 1$], so that

$$\sum_p \mathcal{N}_p \frac{\partial E_p}{\partial \mathcal{N}_n} = N \int dz[\rho_e(z) - \rho_i(z)]\frac{\partial V_z}{\partial \mathcal{N}_n}. \tag{B2}$$

From Eq. (1.43) we get

$$\frac{\partial V_z}{\partial \mathcal{N}_n} = -2\pi e^2 n_s \int dz'|z-z'|\frac{\partial \rho_e(z')}{\partial \mathcal{N}_n}. \tag{B3}$$

Inserting Eq. (B3) into Eq. (B2) yields

$$\begin{aligned}\frac{1}{N}\sum_p \mathcal{N}_p \frac{\partial E_p}{\partial \mathcal{N}_n} &= -2\pi e^2 n_s \int \int dz\ dz'|z-z'|\\ &\qquad \times [\rho_e(z) - \rho_i(z)]\frac{\partial \rho_e(z')}{\partial \mathcal{N}_n}.\end{aligned} \tag{B4}$$

By looking at Eq. (2.19), we see that the right-hand side of Eq. (B4) is equal to $(-\partial E/\partial \mathcal{N}_n)$ so that we have

$$N\frac{\partial E}{\partial \mathcal{N}_n} + \sum_p \mathcal{N}_p \frac{\partial E_p}{\partial \mathcal{N}_n} = 0. \tag{B5}$$

APPENDIX C: $\mathcal{H}_H$ GROUND-STATE ENERGY STARTING FROM AN ARBITRARY $|\mathcal{N}'_1 \cdots \mathcal{N}'_n \cdots\rangle$ STATE

The $\tilde{\mathcal{H}}_0$ Hamiltonian defined in Eq. (2.10) depends on a set of parameters $\mathcal{N}_n$ through the definition of $\rho_e(z)$. Let us consider an N-particle state $|\mathcal{N}'_1 \cdots \mathcal{N}'_n \cdots\rangle$ with $\mathcal{N}'_n$ electrons in the lowest state of the n subband and $\mathcal{N}'_n \neq \mathcal{N}_n$. This state is eigenstate of $\tilde{\mathcal{H}}_0$ with energy

$$\mathcal{E}(\mathcal{N}'_1 \cdots \mathcal{N}'_n \cdots) = \sum_n \mathcal{N}'_n\left[\frac{\pi}{2mS}\mathcal{N}'_n + \tilde{E}_n\right]. \tag{C1}$$

If we look for the $\tilde{\mathcal{H}}_0$ ground state, i.e., for the lowest $\mathcal{E}(\mathcal{N}'_1 \cdots \mathcal{N}'_n \cdots)$ at constant $\mathcal{N}_n$ (which enters $\tilde{E}_n$), we find that it corresponds to $\mathcal{N}'_n = N'_n$ with

$$\gamma = \frac{\pi}{mS}N'_n + \tilde{E}_n, \tag{C2}$$

where γ is a constant (Lagrange) multiplier. We see that N'_n is different from $\mathcal{N}_n$ except when $\mathcal{N}_n$ equals the "equilibrium" filling N_n given by Eq. (2.29). We could be disturbed at first by the fact that the $|\mathcal{N}_1 \cdots \mathcal{N}_n \cdots\rangle$ state we choose to start with (for physical reasons), in Sec. II, is not the $\tilde{\mathcal{H}}_0$ ground state. However we are going to show that, if we start with the $\tilde{\mathcal{H}}_0$ ground state $|N'_1 \cdots N'_n \cdots\rangle$, we do find the same Hartree ground-state energy.

Equation (C2) gives the $\tilde{\mathcal{H}}_0$ ground-state fillings N'_n as functions of the $\mathcal{N}_n$. If we now look for the set of $\mathcal{N}_n$ which minimizes the $\tilde{\mathcal{H}}_0$ ground-state energy, we find that it must verify

$$\gamma' = \frac{\partial \mathcal{E}(N'_1 \cdots N'_n \cdots)}{\partial \mathcal{N}_n}. \tag{C3}$$

Using Eqs. (C1) and (2.28) and remembering that

$$\sum_p N'_p = \sum_p N_p = \sum_p \mathcal{N}_p = N, \tag{C4}$$

we can rewrite Eq. (C3) as

$$\gamma' = \sum_p N'_p \frac{\partial \tilde{E}_p}{\partial \mathcal{N}_n} = \sum_p (N'_p - \mathcal{N}_p)\frac{\partial E_p}{\partial \mathcal{N}_n}. \tag{C5}$$

This shows that $N'_p = \mathcal{N}_p = N_p$ [with N_p the self-consistent solution of Eq. (2.29)] is indeed solution of Eqs. (C2) and (C5). In other words, the $\mathcal{N}'_n$ and $\mathcal{N}_n$ which give the lowest $\tilde{\mathcal{H}}_0$ eigenenergy are such that $\mathcal{N}'_n = \mathcal{N}_n = N_n$.

If we then introduce the $\tilde{\mathcal{V}}^{(q=0)}$ interaction on this lowest $\tilde{\mathcal{H}}_0$ ground state, we find again that the energy is not modified, due to the "magic" relation [Eq. (2.12)], so that $\mathcal{E}(N_1 \cdots N_n \cdots)$ is indeed the exact ground-state energy of the Hartree Hamiltonian.

APPENDIX D: SUMS APPEARING IN THE EXCHANGE ENERGY

Let us consider $J_{nm}(q)$ as defined by Eq. (3.13). For $n=m$, J_{nn} is proportional to the intersection area of two circles with same radius. We find

$$J_{nn}(q) = \begin{cases} \dfrac{SK_n^2}{4\pi^2}\left[2\cos^{-1}\left(\dfrac{q}{2K_n}\right) - \dfrac{q}{K_n}\left[1 - \dfrac{q^2}{4K_n^2}\right]^{1/2}\right] & \text{for } 0 \leqslant q \leqslant 2K_n \\ 0 \ \text{ for } \ q \geqslant 2K_n . \end{cases}$$

For $n \neq m$ the two circles have different radius, and we find

$$J_{12}(q)=\begin{cases} \dfrac{SK_2^2}{4\pi} \text{ for } 0 \leqslant q \leqslant K_1-K_2 \\ \dfrac{SK_1^2}{4\pi^2}\left[\theta+\dfrac{K_2^2}{K_1^2}\theta'-\dfrac{q}{K_1}\sin\theta\right] \text{ for } K_1-K_2 \leqslant q \leqslant K_1+K_2 \\ 0 \text{ for } q \geqslant K_1+K_2 \end{cases}$$

with

$$\theta=\cos^{-1}\left[\frac{q^2+K_1^2-K_2^2}{2qK_1}\right], \quad \theta'=\cos^{-1}\left[\frac{q^2+K_2^2-K_1^2}{2qK_2}\right].$$

---

[1] M. Combescot, O. Betbeder-Matibet, C. Benoit à la Guillaume, and K. Boujdaria, Solid State Commun. **88**, 309 (1993).

[2] O. Betbeder-Matibet, M. Combescot, and C. Tanguy, Phys. Rev. Lett. **72**, 4125 (1994).

[3] W. Kohn and L. J. Sham, Phys. Lett. **140A**, 1133 (1965).

[4] T. Ando and S. Mori, J. Phys. Soc. Jpn. **47**, 1518 (1979).

[5] G. E. W. Bauer and T. Ando, J. Phys. C **19**, 1537 (1986).

[6] G. Eliasson, P. Hawrylak, and J. J. Quinn, Phys. Rev. B **35**, 5569 (1987).

[7] J. C. Ryan, Phys. Rev. B **43**, 12 406 (1991).

[8] J. C. Ryan and T. L. Reinecke, Phys. Rev. B **47**, 9615 (1993).

[9] M. L. Glasser, F. Garcia-Moliner, and V. R. Velasco, Phys. Scr. **43**, 512 (1991).

[10] These subband filling changes were not considered in Refs. 8 and 9.

[11] A Fetter and J. Walecka, *Quantum Theory of Many-Particle Systems* (McGraw-Hill, New York, 1971).

[12] We have set $\hbar=k_B=1$ and $e^2=q^2/4\pi\varepsilon\varepsilon_0$, where q is the electron charge and ε the dielectric constant of the material.

[13] Let us stress that the additional π^{-4} prefactor which comes in Eq. (1.15) and which helps to keep λ_H small, indeed appears in the $\mathscr{V}^{(q=0)}$ expansion of the Hartree energy, as explicitly shown in Ref. 1. With this definition of λ_H, the numerical coefficients of this expansion are of the order of 1.

[14] S. L. Chuang, M. S. C. Luo, S. Schmitt-Rink, and A. Pinczuk [Phys. Rev. B **46**, 1897 (1992)] have also used similar self-consistent $q \neq 0$ matrix elements for the exchange energy in a one-subband filling case. However, in this case, a λ_H expansion of the Hartree terms is quite accurate and such a self-consistent treatment is unnecessary.